Graphical Calculus of Spin Networks

自旋网络图形微积分

Emanuele Alesci, Ilkka Mäkinen, and Jinsong Yang

埃马努埃莱·阿莱希，伊尔卡·迈基宁，杨金松

Contents

目录

E. Alesci (∅)

E. 阿莱奇 (∅)

Institute for Theoretical Physics & Cosmology, Zhejiang University of Technology, Hangzhou, China

中国杭州，浙江工业大学理论物理与宇宙学研究所

United Center for Gravitational Wave Physics (UCGWP), Zhejiang University of Technology, Hangzhou, China

中国杭州，浙江工业大学引力波物理学联合中心 (UCGWP)

I. Mäkinen

I. 迈基宁

National Centre for Nuclear Research, Warsaw, Poland

波兰华沙，国家核研究中心

Faculty of Physics, University of Warsaw, Warsaw, Poland e-mail: ilkka.makinen@ncbj.gov.pl

波兰华沙，华沙大学物理学院电子邮箱:ilkka.makinen@ncbj.gov.pl

J. Yang

杨景

School of Physics, Guizhou University, Guiyang, China

中国贵阳，贵州大学物理学院

e-mail: jsyang@gzu.edu.cn

电子邮箱:jsyang@gzu.edu.cn

Graphical techniques provide a very useful practical device for calculations involving the so-called spin network states, which encode the quantum degrees of freedom of spatial geometry in loop quantum gravity. Graphical calculus of $SU(2)$, which has been originally introduced in the literature in order to deal with calculations arising from the coupling of angular momenta in quantum mechanics, can be used as a simple but powerful method for computing the action of various physically interesting operators in the spin network representation. Compared with conventional manipulation of algebraic expressions, calculations in the graphical approach are typically more convenient, concise, and visually transparent. The goal of this chapter is to provide an accessible introduction to graphical methods in $SU(2)$ recoupling theory and a brief description of their use as a tool for practical calculations in loop quantum gravity. We introduce the basics of the graphical formalism and establish the representation of the elementary states and operators of loop quantum gravity in graphical form. Several example calculations are given to illustrate the use of the graphical techniques, including a computation of the matrix elements of a Hamiltonian constraint operator in the spin network basis.

图形方法是处理自旋网络态相关计算非常实用的工具，自旋网络态在圈量子引力中编码空间几何的量子自由度。$SU(2)$ 图形演算最初是为处理量子力学中角动量耦合相关计算提出的，它是一种简洁且强大的方法，可用于计算自旋网络表示中各类有物理意义的算符的作用。与传统的代数表达式处理相比，图形方法的计算通常更方便、更简洁，也更直观。本章的目的是通俗易懂地介绍 $SU(2)$ 重耦理论中的图形方法，简要说明其作为实用计算工具在圈量子引力中的应用。我们介绍图形形式体系的基础，给出圈量子引力基本态和算符的图形表示，同时通过多个计算示例演示图形技术的用法，其中包括在自旋网络基下计算哈密顿约束算符的矩阵元。

Keywords

关键词

Loop quantum gravity - Graphical calculus - Spin network states - Intertwiners · Hamiltonian constraint operator ·$SU(2)$ representation theory · $SU(2)$ recoupling theory · Angular momentum diagrams

圈量子引力-图形演算-自旋网络态-缠结算子 · 哈密顿约束算符 ·$SU(2)$ 表示论 · $SU(2)$ 重耦合理论 · 角动量图

Introduction

引言

Loop quantum gravity provides a non-perturbative and background-independent approach to the quantization of general relativity (see, e.g., [10,40,44,47] for books and [9, 11, 27, 28, 38, 41, 46] for review articles). The theory incorporates a key lesson of general relativity - that the gravitational field and the geometry of spacetime are essentially the same physical entity - and is built on a rigorous mathematical foundation. In the past 30 years, loop quantum gravity has developed into one of the main candidates for a quantum theory of gravitation, both its canonical (Hamiltonian) and covariant (Lagrangian) formulations.

圈量子引力为广义相对论的量子化提供了一种非微扰且不依赖背景的方法 (相关专著参见例如 [10,40,44,47]，综述文章参见 [9, 11, 27, 28, 38, 41, 46])。该理论吸收了广义相对论的核心结论——引力场与时空几何本质上是同一物理实体，并建立在严谨的数学基础之上。过去 30 年间，圈量子引力已经发展成为量子引力理论的主要候选之一，同时拥有正则 (哈密顿) 表述和协变 (拉格朗日) 表述。

At the heart of loop quantum gravity are the so-called spin network states, which encode the quantum degrees of freedom of discrete, quantized spatial geometries [42, 43]. The use of graphical techniques for calculations involving spin network states has a long history in loop quantum gravity. The articles introducing the spin network representation [42,43] and performing some of the first detailed computations with operators in the spin network basis (e.g., [15,17]) made extensive use of graphical methods which can be traced back to Penrose's diagrammatic tensor calculus [37] and the tangle-theoretic recoupling theory due to Kauffman and Lins [30]. A related but arguably more powerful graphical formalism for $SU(2)$ recoupling theory was originally developed to deal with calculations arising from the coupling of angular momenta in quantum mechanics and has been presented in slightly different versions by Yutsis et al. [56], Brink and Satchler [16], and Varshalovich et al. [49]. All these methods consist of two ingredients: graphical representation and graphical calculation. An algebraic formula involving objects of $SU(2)$ recoupling theory is first represented by a corresponding graphical diagram in a unique and unambiguous way. Then the graphical calculation will be performed following certain simple rules for transforming graphical expressions, which correspond uniquely to algebraic manipulations of the corresponding nongraphical formulae.

圈量子引力的核心是所谓的自旋网络态，它编码了离散量子化空间几何的量子自由度 [42, 43]。在圈量子引力中，使用图形技术对自旋网络态进行计算有着悠久的历史。介绍自旋网络表示 [42,43]、并在自旋网络基下对算符完成首批详细计算 (例如 [15,17]) 的文章就大量使用了图形方法，这些方法可追溯至彭罗斯的张量图解微积分 [37]，以及考夫曼和林斯的扭结理论重耦理论 [30]。另一种与之相关、但能力更强的 $SU(2)$ 重耦理论图形形式，最初是为处理量子力学中角动量耦合产生的计算发展而来，Yutsis 等人 [56]、Brink 和 Satchler[16] 以及 Varshalovich 等人 [49] 分别给出了略有不同的版本。所有这些方法都包含两个部分: 图形表示与图形计算。涉及 $SU(2)$ 重耦理论对象的代数公式首先会以唯一明确的方式表示为对应图形, 之后遵循特定的简单规则对图形表达式进行变换即可完成图形计算，这些变换与非图形公式的代数操作一一对应。

The graphical methods originating from the literature of quantum angular momentum provide a very useful tool for practical calculations in loop quantum gravity. Examples of calculations to which $SU(2)$ graphical calculus has been successfully applied include studying the action of geometric operators (such as the volume operator [8, 42]) [13, 17, 51, 53, 54] and the Hamiltonian constraint operator [4, 6, 7, 26, 35] in the spin network basis; examining the consistency [5, 48, 55] between the dynamics defined by Thiemann's Hamiltonian constraint [45] and the EPRL (Engle-Pereira-Rovelli-Livine) spin foam model [22,24,29]; analysis of the semiclassical limit of the Barrett-Crane spin foam model [3]; and a proof of invariance of a lattice formulation of BF theory under Pachner moves [31]. Pedagogical presentations of these graphical techniques and their use in loop quantum gravity have been given in [34,36].

源自量子角动量领域的图形方法,是圈量子引力实际计算中非常实用的工具。$SU(2)$ 图形微积分已经成功应用于多项计算，包括: 研究几何算符 (例如体积算符 [8, 42]) [13, 17, 51, 53, 54] 和哈密顿约束算符 [4, 6, 7, 26, 35]) 在自旋网络基下的作用；检验蒂曼哈密顿约束定义的动力学 [45] 与 EPRL(Engle-Pereira-Rovelli-Livine) 自旋泡沫模型 [22,24,29] 之间的一致性 [5, 48, 55] ； 分析巴雷特-克兰自旋泡沫模型的半经典极限 [3]；证明 BF 理论的格点表述在帕奇纳移动下不变 [31]。已有文献 [34,36] 对这些图形技术及其在圈量子引力中的应用做了教学性介绍。

Various generalizations and extensions of the graphical method have been developed to extend its reach beyond calculations involving purely $SU(2)$ recoupling theory. In particular, graphical calculus of the group $SL(2,\mathbb{C})$ plays an essential role in the analysis of EPRL spin foam amplitudes (see, e.g., [38] for a review, or the recent articles [19, 20, 25] for a selection of examples). The graphical approach has also been extended to $SU(3)$ in connection with Yang-Mills theory coupled to loop quantum gravity [32], to $OSp(1\mid 2)$ in the context of loop quantum supergravity [33], and to the quantum group $SU(2)_q$ (see, e.g., [14, 18]). Furthermore, graphical techniques been applied to calculations in quantum-reduced loop gravity [1, 2] .

人们已经开发出图形方法的多种推广与扩展，将其应用范围拓展到纯 $SU(2)$ 重耦理论计算之外。尤其是群 $SL(2,\mathbb{C})$ 图形微积分，在分析 EPRL 自旋泡沫振幅中起到核心作用 (例如综述参见 [38]，代表性例子参见近期文章 [19, 20, 25])。图形方法还结合杨-米尔斯理论与圈量子引力耦合的研究拓展到 $SU(3)$ ，在圈量子超引力背景下拓展到 $OSp(1\mid 2)$ ，还拓展到量子群 $SU(2)_q$ (例如参见 [14, 18])。此外，图形技术也已经应用于约化量子圈引力中的计算 [1, 2] 。

Such advanced applications, however, are decidedly outside the scope of our discussion. The purpose of this chapter is limited to giving an accessible introduction to the graphical calculus of $SU(2)$ recoupling theory and explaining how these graphical techniques can be applied to concrete calculations in loop quantum gravity in the spin network representation. After introducing the elements of the graphical formalism in

section ”Elements of Graphical Calculus” and the highly useful fundamental theorem of graphical calculus in section ”Calculating with Graphical Diagrams,” we establish the graphical representation of the elementary states and operators of loop quantum gravity in section ”The Graphical Method in Loop Quantum Gravity” and illustrate their use with an example calculation of the matrix elements of the Hamiltonian constraint operator. The chapter is concluded with a brief summary in section ”Summary.”

然而，这类高级应用显然超出了本文的讨论范围。本章的目的仅限于通俗易懂地介绍 $SU(2)$ 重耦理论的图形计算，讲解这些图形技术如何应用于自旋网络表象下圈量子引力的具体计算。我们会在“图形计算基础”一节介绍图形形式体系的基本要素，在“图形图计算”一节介绍极具实用性的图形计算基本定理，随后在“圈量子引力中的图形法”一节建立圈量子引力基本态和算符的图形表示，并通过计算哈密顿约束算符的矩阵元实例演示它们的用法。本章最后在“总结”一节给出简要总结。

Elements of Graphical Calculus

图形演算基础

In this section, we introduce a diagrammatic notation for the fundamental objects of $SU(2)$ representation theory and establish the basic rules for manipulating such diagrams. The conventions we choose are not in complete agreement with any standard reference on the subject, although they follow quite closely the conventions of Brink and Satchler [16]. Our discussion is interlaced with a concise summary of the necessary elements of $SU(2)$ representation theory, but does not provide a comprehensive review. If necessary, we encourage the reader to consult some of the many available references on Lie groups and the quantum theory of angular momentum (e.g., [16, 21, 23, 50]).

本节我们将为 $SU(2)$ 表示论的基础对象引入图示记法，并建立这类图的基本操作规则。我们选用的约定虽与该主题现有任一标准参考文献都不完全一致，但总体非常贴近 Brink 和 Satchler[16] 的约定。我们的讨论穿插汇总了 $SU(2)$ 表示论的必要基础内容，但并未给出全面综述。如有需要，我们建议读者查阅现有众多关于李群和角动量量子理论的参考资料 (例如 [16, 21, 23, 50])。

SU(2) Representation Theory

SU(2) 表示论

The fundamental representation of $SU(2)$, the group of unitary 2×2 matrices with determinant $+1$, is realized by the natural action of these matrices on $\mathbb{C}^2$. Higher irreducible representations can be described in terms of the states $|jm\rangle$, which are the familiar eigenstates of angular momentum ($|jm\rangle$ is an eigenstate of the operators J^2 and J_z with respective eigenvalues $j(j+1)$ and m) . The spin- j representation of $SU(2)$ is realized on the $(2j+1)$ -dimensional space $\mathcal{H}_j$ spanned by the states $|jm\rangle$ with a fixed value of the quantum number j .

行列式为 +1 的幺正 2×2 矩阵群 $SU(2)$ 的基础表示，由这些矩阵在 $\mathbb{C}^2$ 上的自然作用实现。更高阶的不可约表示可以通过态 $|jm\rangle$ 描述，这些态就是我们熟知的角动量本征态，($|jm\rangle$ 是算符 J^2 和 J_z 的本征态，本征值分别为 $j(j+1)$ 和 m)。$SU(2)$ 的自旋- j 表示实现于由量子数 j 固定的态 $|jm\rangle$ 张成的 $(2j+1)$ 维空间 $\mathcal{H}_j$ 上。

The matrices representing elements of $SU(2)$ on $\mathcal{H}_j$ are known as the Wigner matrices. We denote their matrix elements by

$SU(2)$ 的元素在 $\mathcal{H}_j$ 上的表示矩阵称为维格纳矩阵。我们将其矩阵元记作

$$D^{(j)m}{}_n(g) = \langle jm\,|D^{(j)}(g)|\,jn\rangle. \tag{1}$$

To express these matrix elements in graphical form, we adopt the notation

为了用图形形式表示这些矩阵元，我们采用记号

(2)

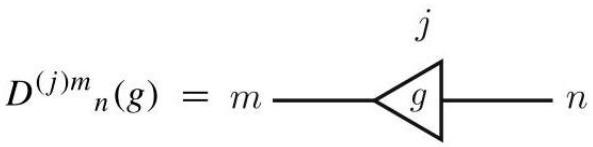

with the tip of the triangle pointing toward the upper index.

三角形的尖端指向 upper 指标。

A fundamental invariant tensor on $\mathcal{H}_j$ (the epsilon tensor) is defined by

$\mathcal{H}_j$ 上的一个基本不变张量 (epsilon 张量) 定义为

$$\varepsilon^{(j)}_{mn} = (-1)^{j-m}\delta_{m,-n},\ \varepsilon^{(j)mn} = (-1)^{j-m}\delta_{m,-n}. \tag{3}$$

Note that we define the tensor with upper indices to be numerically equal to its counterpart with lower indices. From its definition, we see that the epsilon tensor satisfies the properties

注意我们定义带 upper 指标的张量在数值上等于对应的带 lower 指标的张量。从它的定义可以看出，epsilon 张量满足性质

$$\varepsilon^{(j)}_{nm} = (-1)^{2j}\varepsilon^{(j)}_{mn},\ \varepsilon^{(j)}_{mm'}\varepsilon^{(j)m'n} = (-1)^{2j}\delta^n_m. \tag{4}$$

The epsilon tensor can be used to raise and lower indices of vectors on $\mathcal{H}_j$. We choose the convention

epsilon 张量可用于升降 $\mathcal{H}_j$ 上矢量的指标。我们采用约定

$$v^m = \varepsilon^{(j)mn} v_n,\ v_m = v^n \varepsilon^{(j)}_{nm}. \tag{5}$$

The tensor $\varepsilon^{(j)}_{mn}$ is represented graphically by a line carrying an arrow and a label indicating the representation j. The two ends of the line correspond to the indices m and n, with the arrow pointing from m to n :

张量 $\varepsilon^{(j)}_{mn}$ 的图形表示为一条带箭头的线，以及标注表示 j 的标签。线的两端对应指标 m 和 n，箭头从 m 指向 n :

(6)

$$\varepsilon^{(j)}_{mn} \quad = \quad m \xrightarrow{\qquad j \qquad} n.$$

The tensor $\varepsilon^{(j)mn}$, which is numerically equal to $\varepsilon^{(j)}_{mn}$, is represented by the same diagram. We also introduce a line without an arrow to represent the unit tensor (Kronecker delta):

数值上等于 $\varepsilon^{(j)}_{mn}$ 的张量 $\varepsilon^{(j)mn}$ 也用同样的图表示。我们还引入不带箭头的线来表示单位张量 (克罗内克 delta):

(7)

$$\delta^m_n \quad = \quad m \overset{\qquad j \qquad}{\text{———}} n.$$

The properties (4) translate to identities satisfied by the graphical objects (6) and (7). The first property implies that the direction of the arrow can be reversed according to the rule

性质 (4) 转化为图形对象 (6) 和 (7) 满足的恒等式。第一个性质表明，可以按照如下规则反转箭头方向

(8)

$$\xleftarrow{\qquad j \qquad} \quad = \quad (-1)^{2j} \xrightarrow{\qquad j \qquad}.$$

In the graphical formalism, contraction of magnetic indices is represented by connecting the two ends of lines corresponding to the contracted index. The second property (4) then shows that two consecutive arrows behave according to the rules

在图形形式体系中，磁指标的缩并通过连接对应缩并指标的线端来表示。然后性质 (4) 的第二条表明，两个连续箭头遵循如下规则

(9) (10)

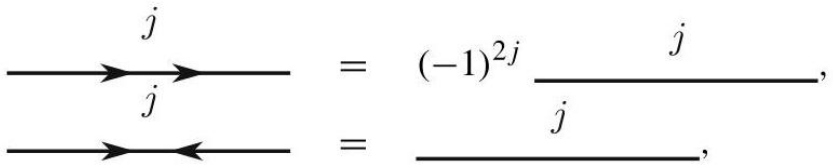

where the second relation is obtained by combining Eqs. (8) and (9).

其中第二个关系式由式 (8) 和 (9) 结合得到。

If the names of the magnetic indices are irrelevant or clear from the context, it is typical to not write the indices explicitly in graphical diagrams such as (6) or (7), as we have already done in Eqs. (8)-(10).

如果磁指标的名称无关紧要或可从上下文看出，通常就不会像我们已经在式 (8)-(10) 中做的那样，在 (6) 或 (7) 这类图形中明确写出指标。

Using the fact that the epsilon tensor is invariant under the action of $SU(2)$ on its indices, one can deduce the expression

利用 epsilon 张量在 $SU(2)$ 作用于其指标下不变这一性质，可以推导出表达式

$$D^{(j)m}{}_{n}\left(g^{-1}\right)=\varepsilon^{(j)mm'}\varepsilon^{(j)}_{nn'}D^{(j)n'}{}_{m'}(g)$$

(11)

for the matrix elements of the inverse matrix $D^{(j)}\left(g^{-1}\right)$ in terms of the matrix $D^{(j)}(g)$. Equivalently, we have the graphical equation

用于表示逆矩阵 $D^{(j)}\left(g^{-1}\right)$ 关于矩阵 $D^{(j)}(g)$ 的矩阵元。等价地，我们有图形方程

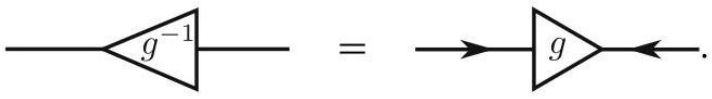

(12)

The great orthogonality theorem for compact groups states that the matrix elements of the Wigner matrices satisfy

紧群的大正交性定理指出，维格纳矩阵的矩阵元满足

$$\int dg\overline{D^{(j)m}{}_{n}(g)}D^{(j')m'}{}_{n'}(g)=\frac{1}{d_j}\delta_{jj'}\delta^{m'}_{m}\delta^{n}_{n'},\tag{13}$$

where dg is the Haar measure of $SU(2)$ and $d_j=2j+1$ is a common abbreviation for the dimension of the space $\mathcal{H}_j$. To express the orthogonality theorem in graphical form, it is convenient to start by using Eq.

(11) together with unitarity, i.e., $D^{(j)}\left(g^{\dagger}\right)=D^{(j)}\left(g^{-1}\right)$, to derive an equation in which the complex conjugate has been removed. Then expressing this equation in graphical notation, one obtains

其中 dg 是 $SU(2)$ 的哈尔测度，$d_j=2j+1$ 是空间 $\mathcal{H}_j$ 维数的常用缩写。为了将正交性定理表示为图论形式，我们可以先结合式 (11) 与幺正性 (即 $D^{(j)}\left(g^{\dagger}\right)=D^{(j)}\left(g^{-1}\right)$) 推导出一个移除了复共轭的方程，再将该方程用图符号表示，即可得到

(14)

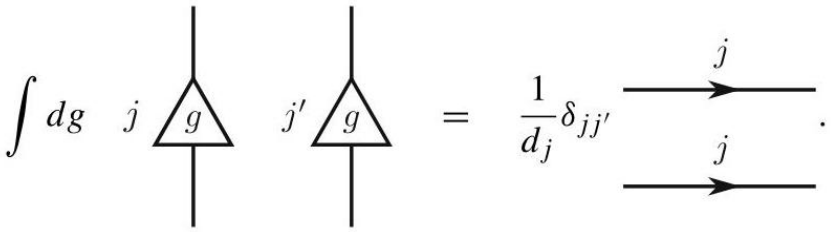

Wigner 3j-symbol

维格纳 3j 符号

Two sets of basis states on the tensor product space $\mathcal{H}_{j_1}\otimes\mathcal{H}_{j_2}$ are given by the "uncoupled" states $|j_1m_1\rangle|j_2m_2\rangle$ and the "coupled" states $|j_1j_2;jm\rangle$, which are defined as the eigenstates of the complete sets of mutually commuting operators $\left\{\left(J^{(1)}\right)^2,J_z^{(1)},\left(J^{(2)}\right)^2,J_z^{(2)}\right\}$ and $\left\{\left(J^{(1)}\right)^2,\left(J^{(2)}\right)^2,\left(J^{(1)}+J^{(2)}\right)^2,J_z^{(1)}+J_z^{(2)}\right\}$. The change of basis between the two bases is given by

张量积空间 $\mathcal{H}_{j_1}\otimes\mathcal{H}_{j_2}$ 上存在两组基矢态，分别是" 未耦合" 态 $|j_1m_1\rangle|j_2m_2\rangle$ 和" 耦合" 态 $|j_1j_2;jm\rangle$，它们分别被定义为对易算子完全集 $\left\{\left(J^{(1)}\right)^2,J_z^{(1)},\left(J^{(2)}\right)^2,J_z^{(2)}\right\}$ 和 $\left\{\left(J^{(1)}\right)^2,\left(J^{(2)}\right)^2,\left(J^{(1)}+J^{(2)}\right)^2,J_z^{(1)}+J_z^{(2)}\right\}$ 的本征态。两组基之间的基变换由下式给出

$$|j_1m_1\rangle|j_2m_2\rangle=\sum_{jm}C^{(j_1j_2j)}{}_{m_1m_2}{}^{m}|j_1j_2;jm\rangle, \tag{15}$$

where $C^{(j_1j_2j)}{}_{m_1m_2}{}^{m}$ are the Clebsch-Gordan coefficients of $SU(2)$. In the physics literature, the Clebsch-Gordan coefficients are usually denoted by a notation such as $\langle j_1m_1,j_2m_2\mid jm\rangle$. The purpose of our notation is to indicate the index structure of the Clebsch-Gordan coefficient when seen as an $SU(2)$ tensor. The phases of the Clebsch-Gordan coefficients are fixed by the nearly universally followed Condon-Shortley convention (see, e.g., [16,21,49]). Under the Condon-Shortley convention, all Clebsch-Gordan coefficients are real-valued, and the coefficients $C^{(j_1j_2j)m_1m_2}{}_{m}$ of the inverse transformation, expressing the coupled states $|j_1j_2;jm\rangle$ in the uncoupled basis, are numerically equal to the coefficients $C^{(j_1j_2j)}{}_{m_1m_2}{}^{m}$ themselves. The Clebsch-Gordan coefficients also feature in the so-called Clebsch-Gordan series

其中 $C^{(j_1 j_2 j)}{}_{m_1 m_2}{}^{m}$ 是 $SU(2)$ 的克莱布希-高登系数。在物理学文献中，克莱布希-高登系数通常采用 $\langle j_1 m_1, j_2 m_2 \mid jm\rangle$ 这类记号表示。我们采用该记号的目的是，当克莱布希-高登系数被视作一个 $SU(2)$ 张量时，可以明确体现它的指标结构。克莱布希-高登系数的相位由几乎得到普遍遵循的康登-肖特利约定确定 (例如参见文献 [16,21,49])。在康登-肖特利约定下，所有克莱布希-高登系数都是实值的；用于以非耦合基表示耦合态 $|j_1 j_2; jm\rangle$ 的逆变换系数 $C^{(j_1 j_2 j)m_1 m_2}{}_{m}$，在数值上与系数 $C^{(j_1 j_2 j)}{}_{m_1 m_2}{}^{m}$ 本身相等。克莱布希-高登系数也出现在所谓的克莱布希-高登级数中

$$D^{(j_1)m_1}{}_{n_1}(g)\, D^{(j_2)m_2}{}_{n_2}(g) = \sum_{jmn} C^{(j_1 j_2 j)m_1 m_2}{}_{m} C^{(j_1 j_2 j)}{}_{n_1 n_2}{}^{n} D^{(j)m}{}_{n}(g)\,, \tag{16}$$

which can be derived by studying how the state (15) transforms under an $SU(2)$ rotation.

这可以通过研究式 (15) 的态在 $SU(2)$ 旋转下的变换方式推导得到。

An object closely related to the Clebsch-Gordan coefficient is the Wigner $3j$ - symbol. The $3j$ -symbol is constructed by using the epsilon tensor to lower the last index of the Clebsch-Gordan coefficient (and multiplying with a numerical factor):

与克莱布希-高登系数密切相关的一个对象是维格纳 $3j$ -符号。该 $3j$ -符号通过利用 epsilon 张量降克莱布希-高登系数的最后一个指标 (再乘以一个数值因子) 构造得到:

$$\begin{pmatrix} j_1 & j_2 & j_3 \\ m_1 & m_2 & m_3 \end{pmatrix} = \frac{1}{\sqrt{d_{j_3}}} (-1)^{j_1 - j_2 + j_3} C^{(j_1 j_2 j_3)}{}_{m_1 m_2}{}^{n} \varepsilon^{(j_3)}_{n m_3}. \tag{17}$$

The value of the $3j$ -symbol is nonvanishing only if the spins j_1, j_2 , and j_3 fulfill the triangular conditions or Clebsch-Gordan conditions

仅当自旋 j_1, j_2 和 j_3 满足三角条件 (即克莱布希-高登条件) 时，$3j$ 符号的值才不为零

$$|j_1 - j_2| \le j_3 \le j_1 + j_2, \text{ and } j_1 + j_2 + j_3 \text{ is an integer,} \tag{18}$$

and the magnetic quantum numbers sum up to zero

且磁量子数总和为零

$$m_1 + m_2 + m_3 = 0 \tag{19}$$

In the graphical notation, the $3j$ -symbol is taken as a fundamental object due to its higher degree of symmetry over the Clebsch-Gordan coefficient. The $3j$ -symbol is represented graphically by a node with three lines connected to it:

在图形记号中，由于 $3j$ -符号比克莱布希-高登系数具有更高的对称性，它被视为基础对象。$3j$ -符号的图形表示为一个连接三条线的节点:

$$\begin{pmatrix} j_1 & j_2 & j_3 \\ m_1 & m_2 & m_3 \end{pmatrix} = j_2 \quad \begin{matrix} j_1 \\ j_3 \\ + \end{matrix} \tag{20}$$

The cyclic order of the spins is indicated by a + or - sign next to the node. The two signs represent, respectively, anticlockwise and clockwise ordering of the spins. Thus, a node with a minus sign represents the $3j$ -symbol

自旋的循环顺序由节点旁的 + 号或-号标记。两个符号分别对应自旋的逆时针顺序和顺时针顺序。因此，带负号的节点代表 $3j$ 符号

$$j_2 = j_3 = \begin{pmatrix} j_1 & j_3 & j_2 \\ m_1 & m_3 & m_2 \end{pmatrix} = j_1 j_2. \tag{21}$$

From Eqs. (17) and (20), it follows that the graphical representation of the Clebsch-Gordan coefficient is given by

由式 (17) 和 (20) 可得，克莱布希-高登系数的图表示为

(22)

$$C^{(j_1 j_2 j)}{}_{m_1 m_2}{}^{m} = (-1)^{j_1 - j_2 - j}\sqrt{d_j}$$

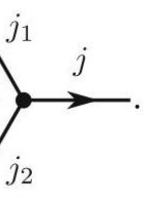

The Clebsch-Gordan series (16) then takes the graphical form

克莱布许-高登级数 (16) 可写成如下图形形式

(23)

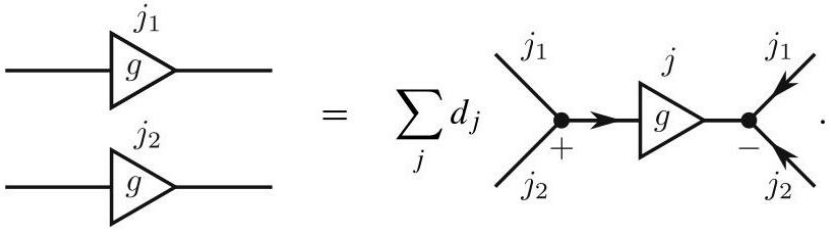

The $3j$ -symbol enjoys a number of convenient symmetry properties. Interchanging any two columns in the symbol is equivalent to multiplying the symbol by $(-1)^{j_1+j_2+j_3}$ (so in particular, the symbol is invariant under cyclic permutations of the columns). The same multiplicative factor results if the sign of all the magnetic numbers is reversed. Translated to graphical notation, these statements imply that the diagram representing the $3j$ -symbol satisfies the following basic properties:

$3j$ 符号具有诸多便捷的对称性。任意交换两列等价于将原符号乘以 $(-1)^{j_1+j_2+j_3}$ (因此该符号在列的循环置换下保持不变)。当所有磁量子数同时变号时，也会得到相同的乘积因子。转换为图形记号后，上述结论意味着代表 $3j$ 符号的图满足以下基本性质:

(24)

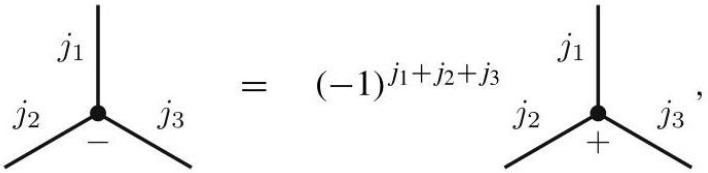

i.e., reversing the sign is equivalent to multiplying the diagram with the phase factor $(-1)^{j_1+j_2+j_3}$, and

即，变号等价于给图乘一个相位因子 $(-1)^{j_1+j_2+j_3}$ ，且

(25)

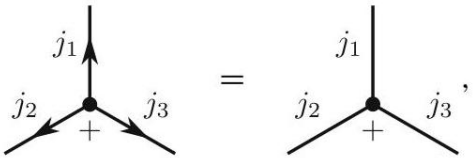

i.e., a node with an identically oriented arrow on each line is equivalent to a node with no arrows. The $3j$ -symbol also satisfies certain orthogonality relations, which encode the orthonormality of the coupled and uncoupled bases and which can be expressed graphically as

即，所有边箭头方向一致的结点等价于不带箭头的结点。$3j$ 符号还满足若干正交关系，这些关系编码了耦合基与非耦合基的标准正交性，可图形化表示为

(27)

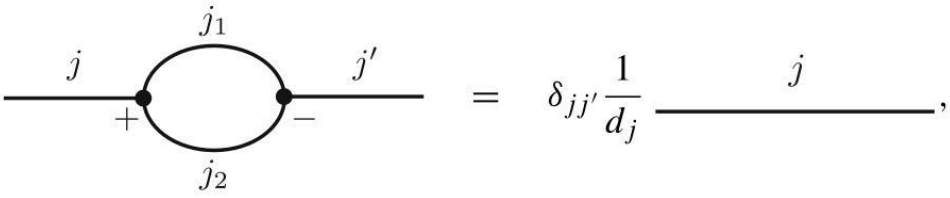

(26)

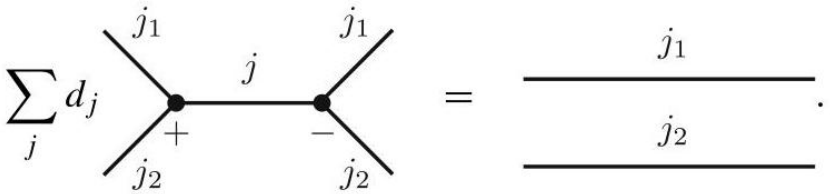

Further properties of the $3j$ -symbol include the identity

$3j$ 符号的其他性质包括如下恒等式

$$+\sum_{j'}^{j} 0 = \delta_{jj'} \frac{1}{\sqrt{d_j}} j \tag{28}$$

which shows how the $3j$ -symbol reduces to the epsilon tensor when one of the spins is equal to zero.

它展示了当其中一个自旋为零时，$3j$ 符号如何退化为 ε 张量。

Certain familiar objects of $SU(2)$ representation theory can be expressed in graphical form by relating them to the $3j$ -symbol. The anti-Hermitian generators $\tau_i^{(j)}$ in the spin- j representation are defined by the matrix elements:

$SU(2)$ 表示论中某些常见对象可以通过关联 $3j$ 符号写成图形形式。自旋- j 表示中的反厄米生成元 $\tau_i^{(j)}$ 由如下矩阵元定义:

$$\left(\tau_i^{(j)}\right)^m{}_n = -i\langle jm\,|J_i|\,jn\rangle. \tag{29}$$

However, the Wigner-Eckart theorem (see, e.g., [16, 21, 49]) states that the matrix elements of the angular momentum operator are given by

但维格纳-埃克特定理 (例如参见文献 [16, 21, 49]) 指出，角动量算符的矩阵元由下式给出

$$\langle jm\,|J_i|\,jn\rangle = (j\,||\,\mathbf{J}\,||\,j)\,C^{(j1j)}{}_{ni}{}^m, \tag{30}$$

where the so-called reduced matrix element $(j\,||\,\mathbf{J}\,\|\,j)$ is independent of the magnetic indices m, n , and i . The value of the reduced matrix element, $\left(j\left\|\mathbf{J}\right\|j\right) = \sqrt{j(j+1)}$, can be deduced, e.g., by considering a complete contraction of Eq. (30) with itself and recalling that the Condon-Shortley convention fixes the sign of the coefficient $C^{(j1j)}{}_{j0}{}^j$ to be positive. In this way one finds that the generators are represented graphically by

其中所谓的约化矩阵元 $(j\,||\,\mathbf{J}\,\|\,j)$ 与磁量子数 m, n 、i 无关。约化矩阵元的值 $\left(j\left\|\mathbf{J}\right\|j\right) = \sqrt{j(j+1)}$ 可以通过例如对式 (30) 做完全缩并，再结合康登-肖特利约定要求系数 $C^{(j1j)}{}_{j0}{}^j$ 的符号为正推导得到。由此我们可以得到生成元的图形表示如下:

(31)

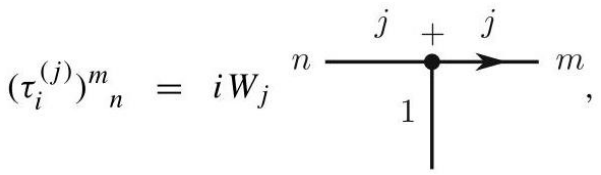

where we have introduced the abbreviation

其中我们引入了如下缩写

$$W_j = \sqrt{j\,(j+1)\,(2j+1)}. \tag{32}$$

Moreover, if we use the diagram

此外，如果我们用下图

(33)

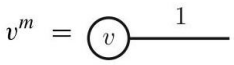

to denote a vector with an index in the $j = 1$ representation, we can write down the expression

表示一个指标属于 $j = 1$ 表示的向量，我们就可以写出表达式

(34)

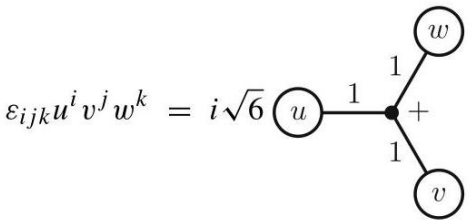

for the triple product of three vectors contracted with the completely antisymmetric tensor ε_{ijk} . This is based on the observation that the $3j$ -symbol with spins $j_1 = j_2 = j_3 = 1$, being antisymmetric under the interchange of any two columns, must be proportional to $\varepsilon_{m_1 m_2 m_3}$, and that a triple product expressed in the Cartesian basis is related to the same product calculated in the spherical basis by $\varepsilon_{ijk}u^i v^j w^k = -i\varepsilon_{m_1 m_2 m_3}u^{m_1}v^{m_2}w^{m_3}$. (The spherical components of a vector $\mathbf{v}$ in $\mathbb{R}^3$ are given in terms of the Cartesian components by $v^+ = -\frac{1}{\sqrt{2}}(v^x - iv^y), v^0 = v^z, v^- = \frac{1}{\sqrt{2}}(v^x + iv^y)$.)

来表示三个向量与全反对称张量 ε_{ijk} 缩并得到的三重积。这一表达基于如下观察: 自旋为 $j_1 = j_2 = j_3 = 1$ 的 $3j$ 符号在任意交换两列时反对称，因此必然正比于 $\varepsilon_{m_1 m_2 m_3}$ ，且笛卡尔基下的三重积和球基下计算的同一三重积差因子 $\varepsilon_{ijk}u^i v^j w^k = -i\varepsilon_{m_1 m_2 m_3}u^{m_1}v^{m_2}w^{m_3}$ 。(向量 $\mathbf{v}$ 在 $\mathbb{R}^3$ 中的球分量可由笛卡尔分量通过 $v^+ = -\frac{1}{\sqrt{2}}(v^x - iv^y), v^0 = v^z, v^- = \frac{1}{\sqrt{2}}(v^x + iv^y)$ 给出。)

Invariant Tensors and Recoupling Theory

不变张量与重耦合理论

In the context of loop quantum gravity, a particularly important property of the $3j$ - symbol is its invariance under $SU(2)$ transformations. With the help of Eq. (16), one can show that

在圈量子引力的语境中，$3j$ 符号的一个尤其重要的性质是它在 $SU(2)$ 变换下的不变性。借助式 (16)，可以证明

$$D^{(j_1)m_1}{}_{n_1}(g)\,D^{(j_2)m_2}{}_{n_2}(g)\,D^{(j_3)m_3}{}_{n_3}(g)\begin{pmatrix} j_1 & j_2 & j_3 \\ m_1 & m_2 & m_3 \end{pmatrix} = \begin{pmatrix} j_1 & j_2 & j_3 \\ n_1 & n_2 & n_3 \end{pmatrix}. \tag{35}$$

A notation such as

我们通常采用如下记号

(36)

$$\iota^{(j_1 j_2 j_3)}_{m_1 m_2 m_3} =$$

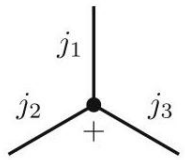

is commonly adopted to denote the $3j$ -symbol if one wishes to emphasize its interpretation as an invariant tensor. The indices of the tensor can be raised with the epsilon tensor in the usual way. In particular, the relation (25) shows that the tensor $\left(\iota^{(j_1 j_2 j_3)}\right)^{m_1 m_2 m_3}$, obtained by raising all the indices of the tensor (36), is numerically equal to $\iota^{(j_1 j_2 j_3)}_{m_1 m_2 m_3}$. Furthermore, the orthogonality relation (26) implies that the tensor (36) is normalized to 1 .

来表示 $3j$ 符号，当我们希望强调它作为不变张量的解释时就会使用这种记法。张量的指标可以按常规方法用 epsilon 张量升标。特别地，关系式 (25) 表明，对张量 (36) 的所有指标升标后得到的张量 $\left(\iota^{(j_1 j_2 j_3)}\right)^{m_1 m_2 m_3}$ 在数值上等于 $\iota^{(j_1 j_2 j_3)}_{m_1 m_2 m_3}$。此外，正交关系 (26) 意味着张量 (36) 归一化为 1。

The $3j$ -symbol and the epsilon tensor are the basic building blocks out of which invariant tensors of higher valence can be constructed. For example, using the epsilon tensor to contract two $3j$ -symbols on one index, we obtain the four-valent invariant tensor

$3j$ 符号和 epsilon 张量是构造更高价不变张量的基础构件。例如，利用 epsilon 张量对两个 $3j$ 符号的一个指标缩并，我们可以得到四价不变张量

(37)

$$\left(\iota^{(j_1 \cdots j_4)}_{k}\right)_{m_1 \cdots m_4} =$$

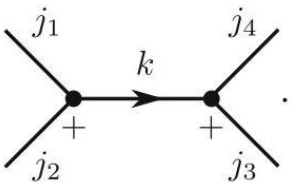

.

From the invariance of the $3j$ -symbol and the epsilon tensor, it follows that the tensor (37) is also invariant under the action of $SU(2)$. Note that invariant tensors whose index structure consists of a mixture of upper and lower indices satisfy $SU(2)$ invariance in the form where a representation matrix acts on each lower index, while the inverse matrix acts on each upper index. For instance, the tensor (37) with the first index raised satisfies

由 $3j$ 符号和 epsilon 张量的不变性可知，张量 (37) 在 $SU(2)$ 的作用下同样是不变的。注意，对于指标结构同时包含上下指标的不变张量，其满足的 $SU(2)$ 不变性形式为: 每个下指标受一个表示矩阵作用，每个上指标则受逆矩阵作用。例如，将第一个指标升标的张量 (37) 满足

$$D^{(j_1)n_1}{}_{m_1}\left(g^{-1}\right) D^{(j_2)m_2}{}_{n_2}(g) \cdots D^{(j_4)m_4}{}_{n_4}(g) \left(\iota_k^{(j_1 \cdots j_4)}\right)^{m_1}{}_{m_2 m_3 m_4} = \left(\iota_k^{(j_1 \cdots j_4)}\right)^{n_1}{}_{n_2 n_3 n_4}. \tag{38}$$

In loop quantum gravity, invariant tensors such as (36) and (37) are typically called intertwiners.

在圈量子引力中，形如 (36) 和 (37) 的不变张量通常被称为交缠子。

The tensors (37) corresponding to all values of the internal spin k allowed by the triangular conditions span the intertwiner space $\mathrm{Inv}\left(\mathcal{H}_{j_1} \otimes \cdots \otimes \mathcal{H}_{j_4}\right)$. However, unlike the three-valent intertwiner (36), the four-valent intertwiners (37) are not normalized; a short calculation using Eq. (26) shows that

所有满足三角条件容许的内部自旋 k 对应的张量 (37) 张成交缠子空间 $\mathrm{Inv}\left(\mathcal{H}_{j_1} \otimes \cdots \otimes \mathcal{H}_{j_4}\right)$。但与三价交缠子 (36) 不同，四价交缠子 (37) 不是归一化的；利用式 (26) 做简单计算可得

(39)

$$\left\langle \iota_k^{(j_1 \cdots j_4)} \middle| \iota_l^{(j_1 \cdots j_4)} \right\rangle =$$

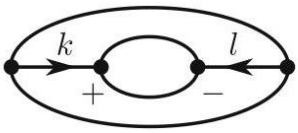

$$= \frac{1}{d_k} \delta_{kl}.$$

Hence, an orthonormal basis on $\mathrm{Inv}\left(\mathcal{H}_{j_1} \otimes \cdots \otimes \mathcal{H}_{j_4}\right)$ is given by the intertwiners

因此，$\mathrm{Inv}\left(\mathcal{H}_{j_1} \otimes \cdots \otimes \mathcal{H}_{j_4}\right)$ 上的标准正交基由如下交缠子给出

$$\left(v_k^{(j_1 \cdots j_4)}\right)_{m_1 m_2 m_3 m_4} = \sqrt{d_k} \left(\iota_k^{(j_1 \cdots j_4)}\right)_{m_1 m_2 m_3 m_4}. \tag{40}$$

The process of using epsilon tensors to connect $3j$ -symbols to each other can be continued to construct intertwiners of arbitrarily high valence. An N -valent intertwiner obtained in this way has the form

我们可以继续用 epsilon 张量连接多个 $3j$ 符号，构造任意高价的交缠子。通过这种方式得到的 N 价交缠子形式为

(41)

$$\iota_{m_1\cdots m_N}^{(k_1\cdots k_{N-3})} =$$

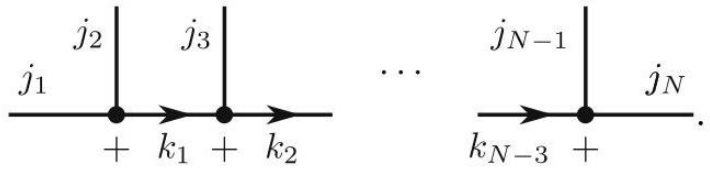

where the label $\mathbf{k}$ denotes the collection of internal spins $k_1, \dots, k_{N-3}$. Seen as a state on $\mathcal{H}_{j_1} \otimes \cdots \otimes \mathcal{H}_{j_N}$, the tensor (41) is an eigenstate of the operators

其中标记 $\mathbf{k}$ 表示内部自旋 $k_1, \dots, k_{N-3}$ 的集合。张量 (41) 看作 $\mathcal{H}_{j_1} \otimes \cdots \otimes \mathcal{H}_{j_N}$ 上的态时，是如下算符的本征态

$$\left(J^{(1)} + J^{(2)}\right)^2,\ \left(J^{(1)} + J^{(2)} + J^{(3)}\right)^2,\ \dots,\ \left(J^{(1)} + J^{(2)} + \cdots + J^{(N-1)}\right)^2$$

(42)

with eigenvalues determined by the spins $k_1, \dots, k_{N-3}, J_N$ and of the operators

其本征值由自旋 $k_1, \dots, k_{N-3}, J_N$ 确定，同时它也是如下算符的本征态

$$\left(J^{(1)} + J^{(2)} + \cdots + J^{(N)}\right)^2,\ J_z^{(1)} + J_z^{(2)} + \cdots + J_z^{(N)} \tag{43}$$

with vanishing eigenvalues. Since these operators form a complete set of commuting operators on $\mathcal{H}_{j_1} \otimes \cdots \otimes \mathcal{H}_{j_N}$, and the invariant subspace $\mathrm{Inv}\left(\mathcal{H}_{j_1} \otimes \cdots \otimes \mathcal{H}_{j_N}\right)$ is characterized by eigenvalues $j = 0$ and $m = 0$ of the total angular momentum, it follows that the states (41) provide a complete basis on the N-valent intertwiner space $\mathrm{Inv}\left(\mathcal{H}_{j_1} \otimes \cdots \otimes \mathcal{H}_{j_N}\right)$ as the internal spins range over all their possible values. As before, this basis is orthogonal but not normalized; an orthonormal basis is given by the intertwiners

具有零本征值。由于这些算符构成 $\mathcal{H}_{j_1} \otimes \cdots \otimes \mathcal{H}_{j_N}$ 上的对易算符完全集，且不变子空间 $\mathrm{Inv}\left(\mathcal{H}_{j_1} \otimes \cdots \otimes \mathcal{H}_{j_N}\right)$ 由总角动量的本征值 $j = 0$ 和 $m = 0$ 刻画，因此当内自旋取遍所有可能值时，态 (41) 给出了 N 价交缠空间 $\mathrm{Inv}\left(\mathcal{H}_{j_1} \otimes \cdots \otimes \mathcal{H}_{j_N}\right)$ 上的一组完备基。和之前一样，该基底正交但未归一化，规范正交基底由如下交缠子给出

$$\left(\upsilon_{\mathbf{k}}^{(j_1\cdots j_N)}\right)_{m_1\cdots m_N} = \sqrt{d_{k_1}\cdots d_{k_{N-3}}}\left(\iota_{\mathbf{k}}^{(j_1\cdots j_N)}\right)_{m_1\cdots m_N}. \tag{44}$$

For intertwiners of valence greater than three, there generally exist many different ways of coupling the spins $j_1, \dots, j_N$ to the internal spins of the intertwiner, giving rise to several inequivalent bases of the corresponding intertwiner space. For example, the intertwiners

对于价数大于三的交缠子，通常存在多种不同方式将自旋 $j_1, \dots, j_N$ 耦合到交缠子的内自旋上，由此得到对应交缠空间的多组不等价基底。例如，以下交缠子

(45)

$$\left(\widetilde{\iota}_l^{(j_1\cdots j_4)}\right)_{m_1\cdots m_4} =$$

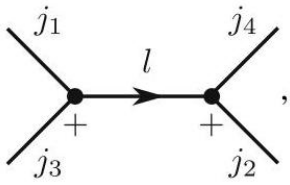

,

where the first and third spins are now coupled to the internal spin, provide another basis of the space $\mathrm{Inv}\left(\mathcal{H}_{j_1}\otimes\cdots\otimes\mathcal{H}_{j_4}\right)$. The change of basis between the bases (37) and (45) is given by

其中第一个和第三个自旋现在耦合到内自旋，给出了空间 $\mathrm{Inv}\left(\mathcal{H}_{j_1}\otimes\cdots\otimes\mathcal{H}_{j_4}\right)$ 的另一组基底。基底 (37) 和 (45) 之间的基变换由下式给出

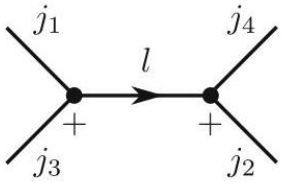

$$= \sum_k d_k(-1)^{j_2+j_3+k+l} \begin{Bmatrix} j_1 & j_2 & k \\ j_4 & j_3 & l \end{Bmatrix}$$

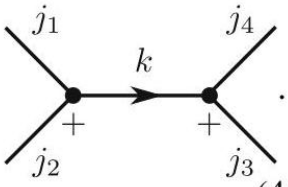

. (46)

Here the object denoted by the curly brackets is a Wigner 6j -symbol. In graphical notation, the 6j-symbol can be defined as the diagram

这里大括号标记的对象是维格纳 6j 符号。在图形记号中，6j 符号可以定义为下图

(47)

$$\begin{Bmatrix} j_1 & j_2 & j_3 \\ k_1 & k_2 & k_3 \end{Bmatrix} =$$

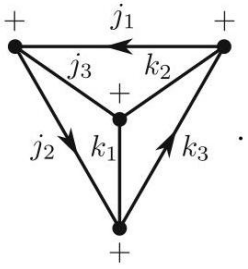

.

(To obtain Eq. (47), contract both sides of Eq. (46) with an intertwiner of the form (37), keeping in mind Eq. (39).) As seen from Eq. (47), the 6j -symbol represents a complete contraction of four 3j -symbols. The 6j -symbol vanishes unless the triangular conditions are satisfied by the four triples of spins indicated by

(要得到式 (47)，将式 (46) 两边与形式为 (37) 的交缠子缩并，记住式 (39) 即可。) 从式 (47) 可以看出，6j 符号代表四个 3j 符号的完全缩并。除非由给出的四组自旋三元组都满足三角条件，否则 6j 符号为零

$$\left\{ \circ\circ\circ \right\} \left\{ \begin{matrix} \circ \\ \end{matrix} \right\} \left\{ \begin{matrix} \circ \\ \circ\circ \end{matrix} \right\} \left\{ \begin{matrix} \circ \\ \circ\circ \end{matrix} \right\}. \tag{48}$$

The symmetry properties of the $6j$ -symbol include invariance under any permutation of its columns

$6j$ 符号的对称性包括其任意列交换下的不变性

$$\left\{ \begin{array}{ccc} j_1 & j_2 & j_3 \\ k_1 & k_2 & k_3 \end{array} \right\} = \left\{ \begin{array}{ccc} j_1 & j_3 & j_2 \\ k_1 & k_3 & k_2 \end{array} \right\} = \left\{ \begin{array}{ccc} j_2 & j_3 & j_1 \\ k_2 & k_3 & k_1 \end{array} \right\}, \text{ etc.} \tag{49}$$

as well as invariance under an interchange of the upper and lower spins in any two columns

以及任意两列中上下自旋交换下的不变性

$$\left\{ \begin{array}{ccc} j_1 & j_2 & j_3 \\ k_1 & k_2 & k_3 \end{array} \right\} = \left\{ \begin{array}{ccc} j_1 & k_2 & k_3 \\ k_1 & j_2 & j_3 \end{array} \right\} = \left\{ \begin{array}{ccc} k_1 & k_2 & j_3 \\ j_1 & j_2 & k_3 \end{array} \right\}, \text{ etc.} \tag{50}$$

Invariant contractions of greater numbers of $3j$ -symbols give rise to higher Wigner nj -symbols. For instance, the change of basis between two bases of five-valent intertwiners is encoded in the $9j$ -symbol, which is a complete contraction of six $3j$ -symbols. These symbols and their properties are described in more detail in references such as [16, 49, 56] .

更多个 $3j$ 符号的不变缩并会产生高阶维格纳 nj 符号。例如，五价交缠子两组基底之间的基变换由 $9j$ 符号刻画，它是六个 $3j$ 符号的完全缩并。这些符号及其性质在 [16, 49, 56] 等参考文献中有更详细的介绍。

Example: The Gauge Invariant Projector

示例: 规范不变投影算子

To give an example of using the elements introduced in this chapter in a concrete calculation, let us consider the integral

为了举例说明如何将本章介绍的内容用于具体计算，我们考虑如下积分

$$I^{(j_1 \cdots j_N)} \equiv \int dg D^{(j_1)}(g) \cdots D^{(j_N)}(g) \,. \tag{51}$$

We would like to show that, seen as an operator on the space $\mathcal{H}_{j_1} \otimes \cdots \otimes \mathcal{H}_{j_N}$, the object (51) represents the orthogonal projector onto the gauge invariant subspace $\mathrm{Inv}\left(\mathcal{H}_{j_1} \otimes \cdots \otimes \mathcal{H}_{j_N}\right)$

我们将证明，将式 (51) 视为作用在空间 $\mathcal{H}_{j_1} \otimes \cdots \otimes \mathcal{H}_{j_N}$ 上的算子时，它对应规范不变子空间 $\mathrm{Inv}\left(\mathcal{H}_{j_1} \otimes \cdots \otimes \mathcal{H}_{j_N}\right)$ 上的正交投影算子

The product of N representation matrices is described graphically by the expression

N 表示矩阵的乘积可以用图形表示为

(52)

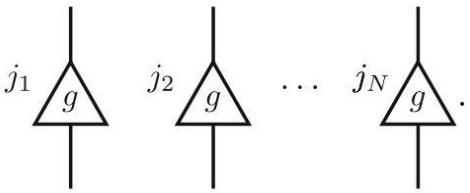

Now the strategy is to repeatedly use Eq. (23) to couple the two leftmost representation matrices. Proceeding in this way until there are only two matrices remaining, we arrive at

现在我们的策略是反复利用式 (23) 耦合最左侧的两个表示矩阵，持续这个过程直到只剩两个矩阵，最终得到

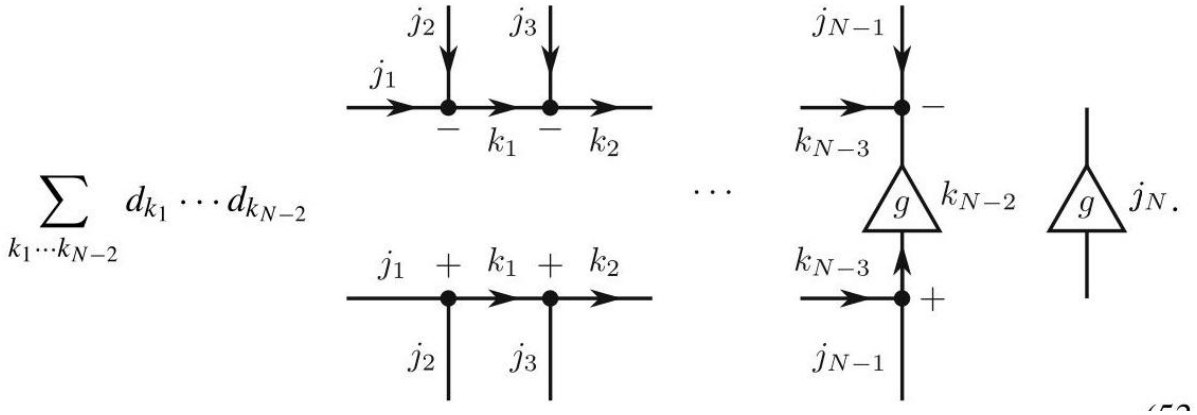

(53)

At this point we may compute the integral over the group using the orthogonality theorem (14) for the Wigner matrices. We then find that the integral (51) is equal to

此时我们可以利用维格纳矩阵的正交性定理 (14) 计算群上的积分，得到积分 (51) 等于

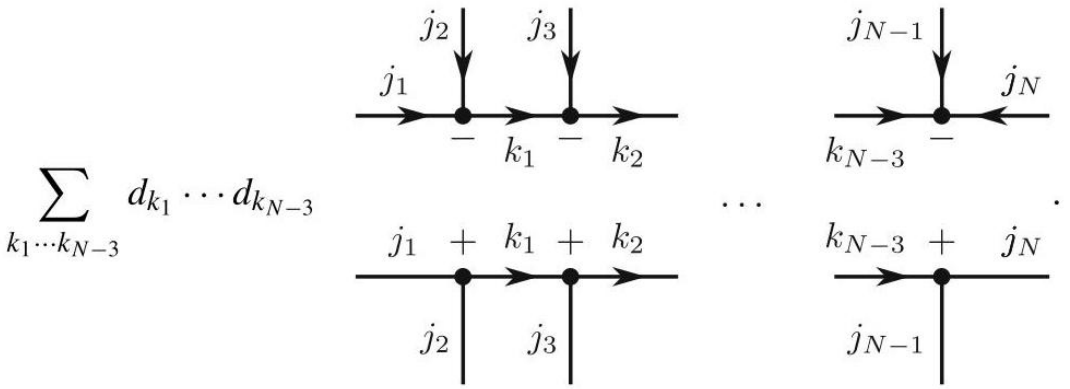

(54)

Here we can recognize the graphical representation of the N -valent intertwiners (41), which span the intertwiner space $\mathrm{Inv}\left(\mathcal{H}_{j_1} \otimes \cdots \otimes \mathcal{H}_{j_N}\right)$. Hence, introducing the label $\mathbf{k}$ to denote the internal spins $k_1, \ldots, k_{N-3}$, we have shown that

这里我们可以认出这是 N 价缠结算子 (41) 的图形表示，这些缠结算子张成缠结算子空间 $\mathrm{Inv}\left(\mathcal{H}_{j_1} \otimes \cdots \otimes \mathcal{H}_{j_N}\right)$。因此，引入标记 $\mathbf{k}$ 表示内自旋 $k_1, \ldots, k_{N-3}$ 后，我们就证明了

$$I^{(j_1 \cdots j_N) m_1 \cdots m_N}{}_{n_1 \cdots n_N} = \sum_{k_1 \cdots k_{N-3}} d_{k_1} \cdots d_{k_{N-3}} \left(\iota_{\mathbf{k}}^{(j_1 \cdots j_N)}\right)^{m_1 \cdots m_N} \left(\iota_{\mathbf{k}}^{(j_1 \cdots j_N)}\right)_{n_1 \cdots n_N}.$$

(55)

Using the normalized intertwiners $\upsilon_{\mathbf{k}}^{(j_1 \cdots j_N)} = \sqrt{d_{k_1} \cdots d_{k_{N-3}}}\, \iota_{\mathbf{k}}^{(j_1 \cdots j_N)}$, we may write

利用归一化缠结算子 $\upsilon_{\mathbf{k}}^{(j_1 \cdots j_N)} = \sqrt{d_{k_1} \cdots d_{k_{N-3}}}\, \iota_{\mathbf{k}}^{(j_1 \cdots j_N)}$ ，我们可以将其写为

$$I^{(j_1 \cdots j_N)} = \sum_{\mathbf{k}} \left|\upsilon_{\mathbf{k}}^{(j_1 \cdots j_N)}\right\rangle \left\langle\upsilon_{\mathbf{k}}^{(j_1 \cdots j_N)}\right|, \tag{56}$$

which establishes the statement we were looking to prove, since Eq. (56) is nothing but the standard way of expressing a projection operator in terms of an orthonormal basis of the subspace onto which the projection is taken.

这就得到了我们想要证明的结论，因为式 (56) 正是投影算子的标准表达形式: 用投影所在子空间的正交基来表示投影算子。

Calculating with Graphical Diagrams

用图形化图解计算

The Fundamental Theorem of Graphical Calculus

图形演算基本定理

In section "Elements of Graphical Calculus" we have introduced the basic ingredients of graphical calculus, consisting of the graphical representation of objects of $SU(2)$ recoupling theory, together with rules such as Eqs. (8)-(10) and (24)-(25) which show how the arrows and signs in graphical diagrams can be manipulated. However, the most powerful element of the graphical method emerges, perhaps surprisingly, from the simple fact that an N -valent invariant tensor can be expanded with respect to a given basis of the corresponding N -valent intertwiner space. Due to their indispensable role in graphical calculations, we will refer to the identities derived from this observation as the fundamental theorem of graphical calculus (although this is not a standard terminology in the literature of the subject). To express these identities in graphical form, we will introduce a notation where an N -valent invariant tensor is represented by a block with N lines attached.

我们在“图形演算基础”一节中介绍了图形演算的基本构成要素，包括 $SU(2)$ 再耦合理论中对象的图形表示，以及式 (8)-(10)、(24)-(25) 这类说明如何操作图形中的箭头和符号的规则。然而，图形方法最强大的作用或许出人意料地来自一个简单事实: 一个 N 价不变张量可以在对应 N 价交缠子空间的给定基下展开。由于这些等式在图形计算中发挥着不可或缺的作用，我们将由该结论推导出的等式称为图形演算基本定理 (尽管这在该领域的文献中并非标准术语)。为了用图形形式表达这些等式，我们引入一种记号: 将 N 价不变张量用一个连接了 N 条线的块表示。

A tensor carrying a single index can be invariant only if the index belongs to the trivial representation. Thus, identifying a line having $j = 0$ with no line, we have

携带单个指标的张量只有当该指标属于平凡表示时才是不变的。因此，若把一条带有 $j = 0$ 的线等同于没有线，我们得到:

(57)

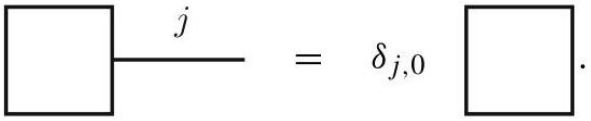

A two-valent invariant tensor T_{mn} must be proportional to $\varepsilon^{(j)}_{mn}$, which is the only invariant tensor having two lower indices. In particular, T_{mn} cannot be invariant unless both of its indices belong to the same representation. The coefficient of proportionality can be deduced by contracting both sides of the equation with the epsilon tensor. In this way we obtain the graphical identity

二价不变张量 T_{mn} 必定与 $\varepsilon^{(j)}_{mn}$ 成正比，$\varepsilon^{(j)}_{mn}$ 是唯一带有两个下指标的不变张量。特别地，除非 T_{mn} 的两个指标属于同一个表示，否则它不可能是不变的。比例系数可以通过对等式两边用 epsilon 张量缩并推导得到，由此我们得到图形恒等式:

(58)

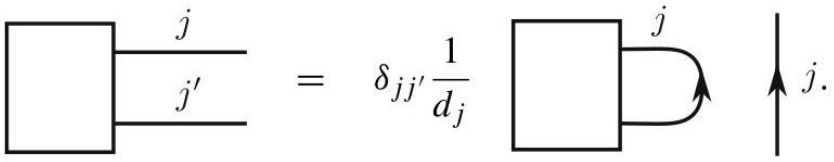

The three-valent intertwiner space $\mathrm{Inv}\left(\mathcal{H}_{j_1} \otimes \mathcal{H}_{j_2} \otimes \mathcal{H}_{j_3}\right)$ is also one-dimensional and is spanned by the $3j$ -symbol (36). A three-valent invariant tensor must therefore be proportional to the $3j$ -symbol, with the coefficient of proportionality determined by contracting both sides of the equation with the $3j$ -symbol:

三价交缠子空间 $\mathrm{Inv}\left(\mathcal{H}_{j_1} \otimes \mathcal{H}_{j_2} \otimes \mathcal{H}_{j_3}\right)$ 也是一维的，由式 (36) 的 $3j$ 符号张成。因此三价不变张量必定与 $3j$ 符号成正比，比例系数由对等式两边用 $3j$ 符号缩并确定:

(59)

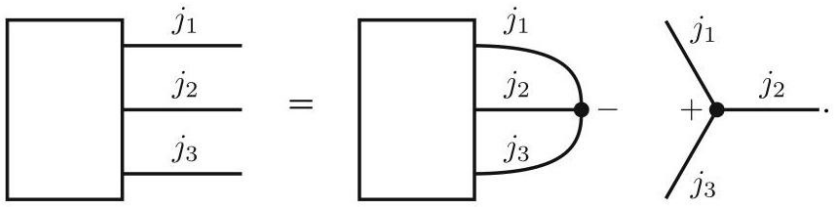

A four-valent invariant tensor can be expanded using any basis of the four-valent intertwiner space $\mathrm{Inv}\left(\mathcal{H}_{j_1} \otimes \cdots \otimes \mathcal{H}_{j_4}\right)$. The dimension of this space is in general higher than 1, so several possible choices of basis are available. If we take the basis given by Eq. (37) and keep in mind the normalization of the basis intertwiners, we can write

四价不变张量可以利用四价交缠子空间 $\mathrm{Inv}\left(\mathcal{H}_{j_1} \otimes \cdots \otimes \mathcal{H}_{j_4}\right)$ 的任意基展开。这个空间的维数通常大于 1，因此存在多种基的选择。如果我们采用式 (37) 给出的基，并牢记基交缠子的归一化，我们可以写出:

(60)

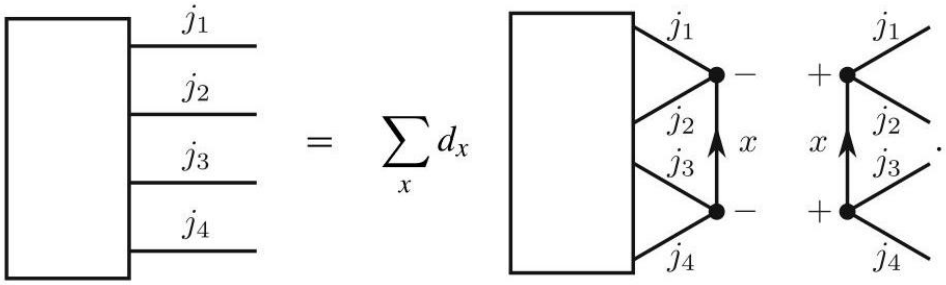

Different versions of the identity (60) can be derived by using different bases of the four-valent intertwiner space. For example, choosing the basis (45), we obtain

通过选用四价交缠子空间的不同基，可以推导出恒等式 (60) 的不同形式。例如，选择基 (45)，我们得到:

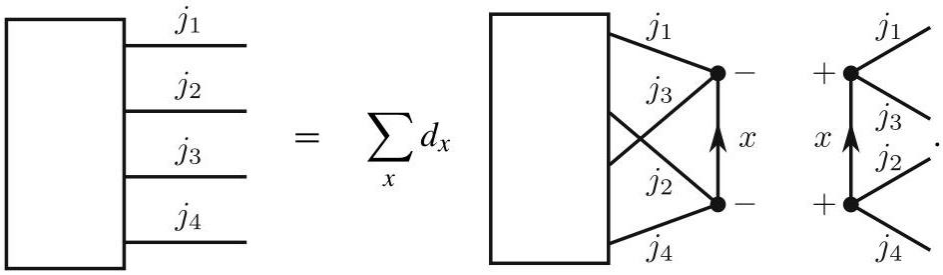

(61)

Invariant tensors of valence higher than four can be expanded in a way completely analogous to Eqs. (60) and (61), using any basis of the appropriate intertwiner space.

价数大于四的不变张量，可以通过选用对应交缠子空间的任意基，以与式 (60)、(61) 完全类似的方式展开。

An important use of the fundamental theorem of graphical calculus is to simplify graphical diagrams which carry no external, uncontracted lines and which therefore represent invariant contractions of $3j$ -symbols. (If the invariance of a given closed diagram constructed out of $3j$ -symbols and epsilon tensors is not immediately apparent, it can be checked by the following criterion: The diagram is invariant if and only if Eqs. (10) and (25) can be used to transform it to a form where each line carries exactly one arrow.) Suppose that an invariant diagram contains a subdiagram which itself represents an N -valent invariant tensor and that the entire diagram can be divided into two disconnected pieces by cutting the N external lines of the subdiagram. In such a case the diagram can be simplified (or at least transformed into a different form) by applying the fundamental theorem to the N - valent intertwiner corresponding to the subdiagram. For diagrams which can be separated into two pieces by cutting one, two, three, or four lines, this procedure gives rise to the following graphical identities:

图形演算基本定理的一个重要应用是化简不带有外部未缩并线、表示 $3j$ 符号不变缩并的图形。(如果由 $3j$ 符号和 epsilon 张量构造出的闭合图的不变性不能直接看出，可以通过以下判据检验: 当且仅当可以用式 (10) 和 (25) 将图变换为每条线恰好带一个箭头的形式时，图是不变的。) 假设一个不变图包含一个本身表示 N 价不变张量的子图，且切断该子图的 N 条外部线后，整个图可以分成两个不连通的部分。在这种情况下，可以通过对该子图对应的 N 价交缠子应用基本定理来化简图 (或至少将其变换为另一种形式)。对于切断 1 条、2 条、3 条或 4 条线就能分成两部分的图，该过程给出以下图形恒等式:

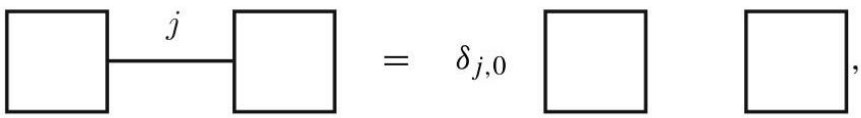

(62)

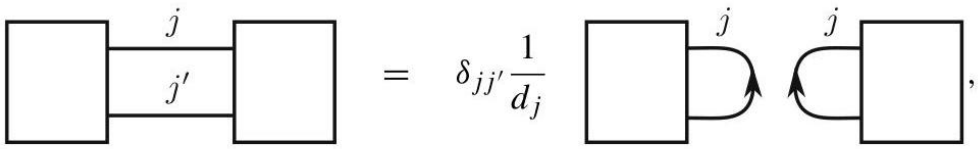

(63)

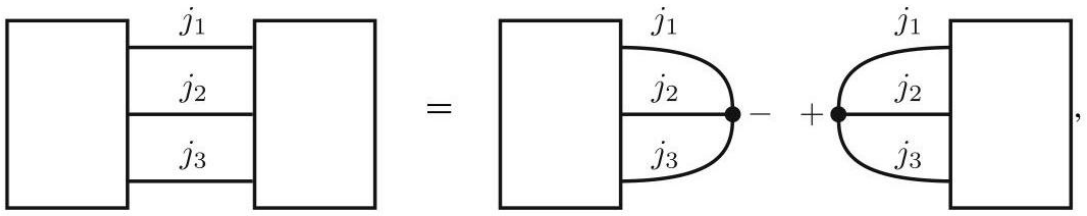

(64)

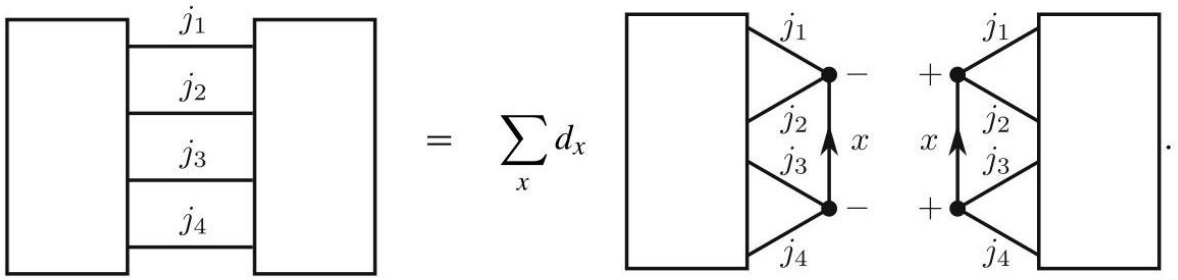

(65)

As before, different versions of Eq. (65) can be obtained by selecting different bases on the four-valent intertwiner space. Equation (65) also generalizes in a straightforward way to the case of cutting a diagram across more than four lines.

和之前的情况一样，通过选择四价交缠子空间的不同基，可以得到式 (65) 的不同形式。式 (65) 也可以直接推广到切断超过四条线的情况。

Example: Biedenharn-Elliot Identity

例题: 比登哈恩-埃利奥特恒等式

An instructive example of using the fundamental theorem of graphical calculus is provided by a graphical proof of the Biedenharn-Elliot identity:

图形微积分基本定理的一个具有启发性的应用实例，就是对比登哈恩-埃利奥特恒等式的图形证明:

$$\begin{Bmatrix} j_1 & j_2 & j_3 \\ k_1 & k_2 & k_3 \end{Bmatrix}\begin{Bmatrix} j_1 & j_2 & j_3 \\ l_1 & l_2 & l_3 \end{Bmatrix}$$

$$= \sum_x d_x (-1)^{j_1+j_2+j_3+k_1+k_2+k_3+l_1+l_2+l_3+x} \begin{Bmatrix} j_1 & k_2 & k_3 \\ x & l_3 & l_2 \end{Bmatrix} \begin{Bmatrix} k_1 & j_2 & k_3 \\ l_3 & x & l_1 \end{Bmatrix} \begin{Bmatrix} k_1 & k_2 & j_3 \\ l_2 & l_1 & x \end{Bmatrix}.$$

(66)

In loop quantum gravity, the Biedenharn-Elliot identity is relevant to the Ponzano-Regge model [12, 39], a spin foam quantization of three-dimensional Euclidean gravity, where it can be used to show that the partition function of the model is invariant under the so-called 2-3 Pachner move.

在圈量子引力中，比登哈恩-埃利奥特恒等式与庞扎诺-雷格模型 [12, 39] 相关，该模型是三维欧几里得引力的自旋泡沫量子化；在这一模型中，可以用该恒等式证明其配分函数在所谓的帕克纳 2-3 移动下保持不变。

We begin from the left-hand side of Eq. (66), using Eq. (47) to express the $6j$ - symbols in graphical form. For the second $6j$ -symbol, we invoke the following theorem about closed diagrams: The value of a diagram representing an invariant contraction of $3j$ -symbols is preserved if all the signs and all the arrows in the diagram are simultaneously reversed. (The proof of this statement is straightforward. After the invariant diagram has been put into a form where each line carries an arrow, reversing all the arrows produces the factor $(-1)^{2J}$, where J is the sum of all the spins in the diagram. Reversing the sign at a node with spins j_1, j_2 and j_3 multiplies the diagram by $(-1)^{j_1+j_2+j_3}$, so reversing all the signs also produces the factor $(-1)^{2J}$, since every line is connected to exactly two nodes. The total factor arising from the process is therefore $(-1)^{4J} = +1$.) Thus, we have a triple of outwardly oriented arrows, as shown by Eq. (25), on each of the three nodes carrying a $+$ sign in order to ensure that each piece resulting from the cut will represent a proper invariant contraction. We then obtain

我们从式 (66) 的左侧出发，利用式 (47) 将 $6j$ 符号表示为图形形式。对于第二个 $6j$ 符号，我们引用下述关于闭合图的定理: 若同时反转图中所有符号和所有箭头，代表 $3j$ 符号不变收缩的图，其值保持不变。(该结论的证明很直接: 当不变图整理为每条线都带一个箭头的形式后，反转所有箭头会得到因子 $(-1)^{2J}$ ，其中 J 是图中所有自旋的和。在带有自旋 j_1, j_2 和 j_3 的节点反转符号，会给图乘上因子 $(-1)^{j_1+j_2+j_3}$ ，因此反转所有符号也会得到因子 $(-1)^{2J}$ ，因为每条线恰好连接两个节点。因此该过程得到的总因子就是 $(-1)^{4J} = +1$ 。) 由此，我们得到如式 (25) 所示、三个向外定向的箭头，分别位于三个带正号的节点上，以保证切割得到的每一块都代表正确的不变收缩。于是我们得到

$$\begin{Bmatrix} j_1 & j_2 & j_3 \\ k_1 & k_2 & k_3 \end{Bmatrix} \begin{Bmatrix} j_1 & j_2 & j_3 \\ l_1 & l_2 & l_3 \end{Bmatrix} =$$

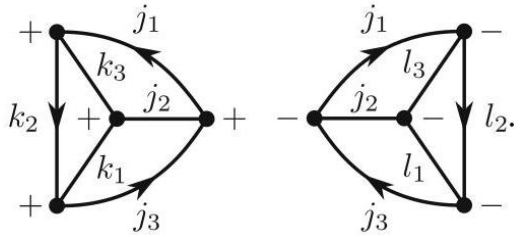

(67)

Now we can see that the structure of the graphical diagram matches with the pattern on the right-hand side of Eq. (64). We may therefore use the fundamental theorem "in reverse" to join the two $6j$ -symbols into a single connected diagram as follows:

现在可以看到，这个图形的结构与式 (64) 右侧的形式一致。因此我们可以“反向”使用基本定理，将两个 $6j$ 符号连接为单个连通图，如下所示:

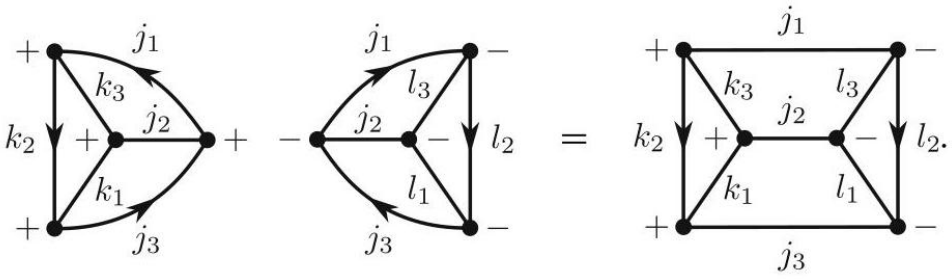

(68)

(After forming the connected diagram we have noted that, as shown by Eq. (10), the two oppositely oriented arrows cancel on the lines carrying spins j_1 and j_3 .)

(构造连通图后我们注意到，如式 (10) 所示，在带有自旋 j_1 和 j_3 的线上，两个方向相反的箭头相互抵消。)

The next step will be to cut the diagram on the right-hand side across four lines, using the fundamental theorem in the form (65). Before doing so, we introduce

下一步，我们利用形如式 (65) 的基本定理，对右侧的图沿四条线切割。在此之前，我们先引入

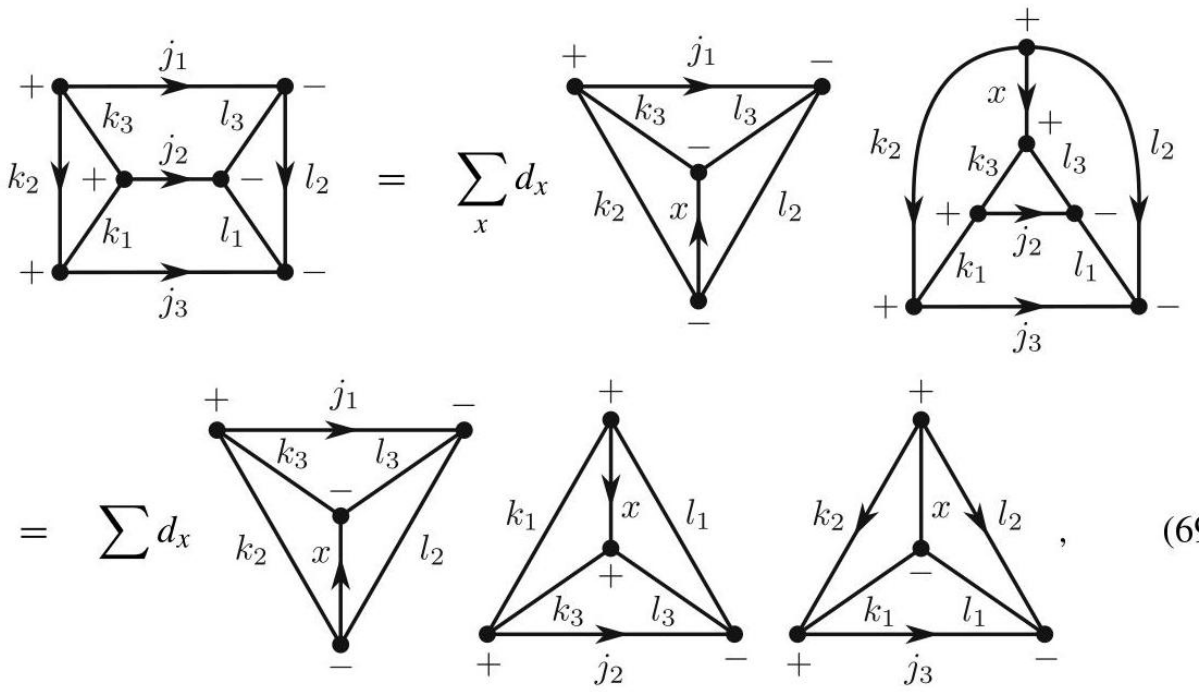

where we have first applied Eq. (65) to cut the diagram across the lines carrying spins k_2, k_3, l_2 , and l_3 and then used the fundamental theorem again to split the new diagram in two pieces by cutting the three

lines that connect the inner part of the diagram to the outer part. Now each diagram on the second line of Eq. (69) can be recognized as a $6j$ -symbol by comparing with the reference diagram (47), adjusting the signs and arrows as needed. (It is useful to remember that simultaneously reversing all the signs and all the arrows does not change the value of a diagram.) For instance, the first diagram is equal to

这里我们首先应用式 (65) 沿带自旋 k_2, k_3, l_2 和 l_3 的线切割图，随后再次利用基本定理，沿连接图内部与外部的三条线切割，将新图拆分为两块。现在，通过与参考图 (47) 对比，在必要时调整符号和箭头，即可认出式 (69) 第二行的每个图都是 $6j$ 符号。(记住同时反转所有符号和所有箭头不会改变图的值，这一点很有用。) 例如，第一个图等于

$$(-1)^{j_1+k_2+k_3}(-1)^{2k_2}\begin{Bmatrix} j_1 & k_2 & k_3 \\ x & l_3 & l_2 \end{Bmatrix}. \tag{70}$$

To obtain the identity (66), it only remains to carefully keep track of the factors of (-1) , noting that the triangular conditions satisfied by the triples (k_1, l_1, x) and (k_2, l_2, x) imply that $(-1)^{2k_1+2l_1+2x} = 1$ and $(-1)^{2k_2+2l_2+2x} = 1$.

要得到恒等式 (66)，我们只需要仔细跟踪 (-1) 的因子，注意到三元组 (k_1, l_1, x) 和 (k_2, l_2, x) 满足的三角条件蕴含 $(-1)^{2k_1+2l_1+2x} = 1$ 和 $(-1)^{2k_2+2l_2+2x} = 1$ 。

The Graphical Method in Loop Quantum Gravity

圈量子引力中的图解法

Kinematical States and Elementary Operators

运动学态与基本算符

The kinematical Hilbert space of loop quantum gravity is spanned by the (generalized) spin network states. A generalized spin network state is labeled by an oriented graph γ together with a set of spins $\mathbf{j} = \{j_1, \dots, j_{N_e}\}$ associated with the edges of the graph and a set of $SU(2)$ tensors (generalized intertwiners) $\boldsymbol{\iota} = \{\iota_1, \dots, \iota_{N_v}\}$ associated with the vertices of the graph (here N_e and N_v denote the number of edges and vertices of the graph). The state is a function of N_e $SU(2)$ group elements and is defined by

圈量子引力的运动学希尔伯特空间由 (广义) 自旋网络态张成。一个广义自旋网络态由定向图 γ 、一组关联于图边的自旋 $\mathbf{j} = \{j_1, \dots, j_{N_e}\}$ 以及一组关联于图顶点的 $SU(2)$ 张量 (广义交缠子) $\boldsymbol{\iota} = \{\iota_1, \dots, \iota_{N_v}\}$ 标记 (此处 N_e 和 N_v 分别表示图的边数与顶点数)。该态是 N_e $SU(2)$ 群元的函数，定义为

$$T_{\gamma,\mathbf{j},\boldsymbol{\iota}}\left(h_{e_1}, \dots, h_{e_N}\right) = \bigotimes_{v\in V(\gamma)} \iota_v \cdot \bigotimes_{e\in E(\gamma)} D^{(j_e)}(h_e). \tag{71}$$

The index structure of the tensor ι_v at a given vertex is adapted to the structure edges incident to the vertex: If the vertex contains M edges oriented outward and labeled by spins $j_1, \dots, j_M$ and $N - M$ edges oriented inward and labeled by spins $j_{M+1}, \dots, j_N$, the tensor ι_v carries M upper indices in the representations

$j_1, \ldots, j_M$ and $N-M$ lower indices in the representations $j_{M+1}, \ldots, j_N$. The dot in Eq. (71) denotes a complete contraction of magnetic indices between the representation matrices and the generalized intertwiners. By restricting the set of tensors ι_v at each vertex to be the invariant tensors (proper intertwiners) described in section "Invariant Tensors and Recoupling Theory," one obtains the proper spin network states, which are invariant under local $SU(2)$ gauge transformations - see Eq. (74) - and which form a basis on the gauge-invariant Hilbert space of loop quantum gravity.

给定顶点处张量 ι_v 的指标结构适配于入射到该顶点的边结构: 若该顶点有 M 条向外取向、标记自旋为 $j_1, \ldots, j_M$ 的边, 以及 $N-M$ 条向内取向、标记自旋为 $j_{M+1}, \ldots, j_N$ 的边, 则张量 ι_v 在表示 $j_1, \ldots, j_M$ 下携带 M 个上指标，在表示 $j_{M+1}, \ldots, j_N$ 下携带 $N-M$ 个下指标。式 (71) 中的点表示表示矩阵与广义交缠子之间磁指标的完全缩并。若将每个顶点处的张量集合 ι_v 限定为“不变张量与重耦理论”小节中描述的不变张量 (正则交缠子), 即可得到正则自旋网络态; 这类态在局域 $SU(2)$ 规范变换下不变 (见式 (74))，并且构成圈量子引力规范不变希尔伯特空间的一组基。

The group elements in Eq. (71) originate classically from holonomies of the Ashtekar connection along curves in the spatial manifold $\sum$. Given an edge $e : [0,1] \to \sum$, the holonomy of the Ashtekar connection A_a^i along the edge is

式 (71) 中的群元经典起源于空间流形 $\sum$ 上沿曲线的阿西特卡联络和乐。给定边 $e : [0,1] \to \sum$ ，沿该边的阿西特卡联络 A_a^i 的和乐为

$$h_e[A] = \mathcal{P} \exp\left(-\int_e A\right)$$

$$= \mathbb{1} + \sum_{n=1}^{\infty} (-1)^n \int_0^1 dt_1 \int_0^{t_1} dt_2 \ldots \int_0^{t_{n-1}} dt_n A(e(t_1)) \cdots A(e(t_n)),$$

(72)

where $A(e(t)) \equiv \dot{e}^a(t) A_a^i(e(t)) \tau_i$, with $\dot{e}^a(t)$ being the tangent vector of e , and $\mathcal{P}$ exp denotes the path ordered exponential, with the largest path parameter ordered to the left. The holonomy satisfies certain properties which reflect its geometric interpretation as a parallel propagator. Perhaps the most important of these is the identity

其中 $A(e(t)) \equiv \dot{e}^a(t) A_a^i(e(t)) \tau_i$ ， $\dot{e}^a(t)$ 是 e 的切向量，$\mathcal{P}$ exp 表示路径序指数，路径参数越大越靠左排列。和乐满足反映其作为平行传播子几何诠释的若干性质，其中最重要的恒等式是

$$h_{e_2 \circ e_1} = h_{e_2} h_{e_1}, \tag{73}$$

where e_1 and e_2 are two edges such that the endpoint of e_1 coincides with the beginning point of e_2 and $e_2 \circ e_1$ is the combined path formed by e_1 followed by e_2 .

其中 e_1 和 e_2 是两条边，满足 e_1 的终点与 e_2 的起点重合，$e_2 \circ e_1$ 是 e_1 后接 e_2 组成的复合路径。

Under a local $SU(2)$ gauge transformation described by a gauge function $g(x) \in SU(2)$, the connection behaves as $A_a \to (A^g)_a \equiv g A_a g^{-1} + g \partial_a g^{-1}$. This implies the corresponding transformation law of the holonomy as

在由规范函数 $g(x) \in SU(2)$ 描述的局域 $SU(2)$ 规范变换下，联络满足变换规则 $A_a \to (A^g)_a \equiv gA_ag^{-1} + g\partial_a g^{-1}$，由此可推导出和乐对应的变换定律为

$$h_e[A^g] = g(f(e))\, h_e[A]\, g^{-1}(b(e)), \tag{74}$$

where $b(e)$ and $f(e)$ denote the beginning and final points of e. Equation (74) suggests that the indices m and n of the representation matrix $D^{(j)m}{}_n(h_e[A])$ are associated respectively with the final and beginning points of the edge e. Our convention for the graphical representation of the Wigner matrices, given by Eq. (2), has been chosen accordingly so that the direction of the triangle is consistent with the orientation of the edge in the holonomy $h_e[A]$.

其中 $b(e)$ 和 $f(e)$ 分别表示 e 的起点和终点。式 (74) 表明，表示矩阵 $D^{(j)m}{}_n(h_e[A])$ 的指标 m 和 n 分别对应边 e 的终点和起点。我们据此选定了式 (2) 给出的维格纳矩阵图形表示约定，使三角形方向与全绕 $h_e[A]$ 中边的方向一致。

The elementary operators of loop quantum gravity are the holonomy and flux operators. The holonomy operator acts as a multiplicative operator:

圈量子引力的基本算符是全绕算符和通量算符。全绕算符以乘法算符的形式作用:

$$\widehat{D^{(j)m}}n(h_e)\, T_{\gamma,\mathbf{j},\iota}(h_{e_1},\dots,h_{e_N}) = D^{(j)m}{}_n(h_e)\, T_{\gamma,\mathbf{j},\iota}(h_{e_1},\dots,h_{e_N}). \tag{75}$$

If the edge e coincides with one of the edges $e_1,\dots,e_N$, the action of the holonomy operator on a spin network state involves essentially the decomposition of the tensor product of two representations, which is given by the Clebsch-Gordan series (16).

若边 e 与某条边 $e_1,\dots,e_N$ 重合，全绕算符对自旋网络态的作用本质上涉及两个表示的张量积分解，该分解由克莱布希-高登级数 (16) 给出。

The flux operator arises as a quantization of the classical variable representing the flux of the densitized triad E^a_i through a two-dimensional surface. The action of the flux operator on a spin network state can be expressed as a linear combination of the left- and right-invariant vector fields of $SU(2)$. The left- and right-invariant vector fields act according to the definitions

通量算符是经典变量的量子化结果，该经典变量描述密化三矢 E^a_i 穿过二维曲面的通量。通量算符对自旋网络态的作用可表示为 $SU(2)$ 左不变向量场和右不变向量场的线性组合。左不变与右不变向量场按照如下定义作用

$$\hat{L}^{(e)}_i T_{\gamma,\mathbf{j},\mathbf{l}}(h_{e_1},\dots,h_{e_N}) = i\frac{d}{dt}\Big|_{t=0} T_{\gamma,\mathbf{j},\mathbf{l}}(h_{e_1},\dots,h_e e^{t\tau_i},\dots h_{e_N}), \tag{76}$$

$$\hat{R}^{(e)}_i T_{\gamma,\mathbf{j},t}(h_{e_1},\dots,h_{e_N}) = -i\frac{d}{dt}\Big|_{t=0} T_{\gamma,\mathbf{j},t}(h_{e_1},\dots,e^{t\tau_i}h_e,\dots h_{e_N}), \tag{77}$$

where the superscripts indicate that the operators act on the argument h_e of the function $T_{\gamma,\mathbf{j},\iota}\left(h_{e_1},\ldots,h_{e_N}\right)$. If these operators are applied on the Wigner matrices themselves, it is immediate to see that their action is given by

其中上标表示算符作用在函数 $T_{\gamma,\mathbf{j},\iota}\left(h_{e_1},\ldots,h_{e_N}\right)$ 的自变量 h_e 上。不难看出，若这些算符直接作用在维格纳矩阵上，其作用结果为

$$\hat{L}_i^{(e)} D^{(j)}\left(h_e\right) = iD^{(j)}\left(h_e\right)\tau_i^{(j)}, \tag{78}$$

$$\hat{R}_i^{(e)} D^{(j)}\left(h_e\right) = -i\tau_i^{(j)} D^{(j)}\left(h_e\right). \tag{79}$$

To apply the methods of graphical calculus for calculations in loop quantum gravity, the general strategy is as follows. Firstly, one expresses the spin network states in a graphical form. Secondly, one derives graphically the action of the two elementary operators on the spin network states. After this has been done, the action of any well-defined operator constructed out of the elementary operators can be derived by applying the graphical formalism introduced in sections "Elements of Graphical Calculus" and "Calculating with Graphical Diagrams."

在圈量子引力中应用图形计算方法的一般策略如下: 首先，将自旋网络态表示为图形形式；其次，用图形方法推导出两个基本算符对自旋网络态的作用；完成这两步后，任何由基本算符构造得到的良定义算符的作用，都可以通过应用“图形计算基础”和“图形 diagram 计算”两节中介绍的图形形式体系推导出来。

The spin network states defined by Eq. (71) involve two ingredients: the representation matrices $D^{(j)}\left(h_e\right)$ and the intertwiners ι_v. The graphical representation of the Wigner matrices is given by Eq. (2), while the graphical representation of intertwiners has been discussed in section "Invariant Tensors and Recoupling Theory." Let $T^v_{\gamma,\mathbf{j},\iota}$ denote the part of a spin network state directly associated with the vertex v. Assume that the vertex v contains N edges $e_1,\ldots,e_N$, the first M of which are oriented outward and the remaining $N-M$ are oriented inward. If the intertwiner at v is a tensor of the form (41), the function $T^v_{\gamma,\mathbf{j},\iota}$ is represented graphically by the expression

式 (71) 定义的自旋网络态包含两个组成部分: 表示矩阵 $D^{(j)}\left(h_e\right)$ 和 intertwiner ι_v。维格纳矩阵的图形表示由式 (2) 给出，而 intertwiner 的图形表示已在“不变张量与重耦合理论”一节中讨论。设 $T^v_{\gamma,\mathbf{j},\iota}$ 是自旋网络态中直接对应顶点 v 的部分，假设顶点 v 包含 N 条边 $e_1,\ldots,e_N$，其中前 M 条边向外定向，剩余 $N-M$ 条边向内定向。若 v 处的 intertwiner 是形如 (41) 的张量，则函数 $T^v_{\gamma,\mathbf{j},\iota}$ 的图形表示为

$T^v_{\gamma,\mathbf{j},\iota}(h_{e_1},\ldots,h_{e_N}) =$

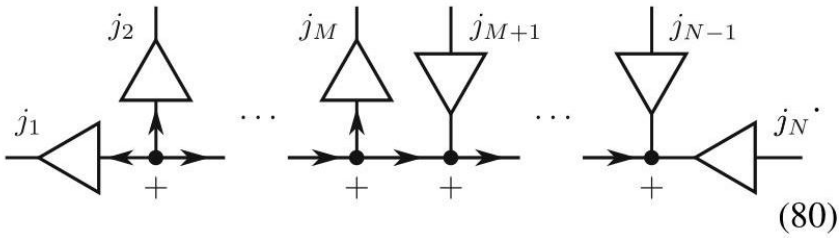

(80)

Note that, for each edge oriented outward, the corresponding index of the intertwiner has been raised using the epsilon tensor.

注意，对每条向外定向的边，我们已利用 ε 张量提升了 intertwinner 对应指标的位置。

Now let us consider the graphical calculation of the action of the two elementary operators on spin network states. The action of the holonomy operator is encoded in the Clebsch-Gordan series, which is given in algebraic form by Eq. (16) and in graphical form by Eq. (23). Applying the holonomy operator to the state (80), and using Eq. (23) to evaluate the resulting action, we find that the action of the holonomy operator can be represented in graphical form as

现在我们考虑两个基本算符作用在自旋网络态上的图形计算。全绕算符的作用包含在克莱布希-高登级数中，该级数的代数形式由式 (16) 给出，图形形式由式 (23) 给出。将全绕算符作用于态 (80)，再利用式 (23) 计算得到的作用，我们发现全绕算符的作用可以用图形形式表示为

$$D^{(j)\widehat{m_n(h_e)}} T^{v}_{\gamma \mathbf{j},\mathbf{t}}\left(h_{e_1},\dots,h_e,\dots,h_{e_N}\right)$$

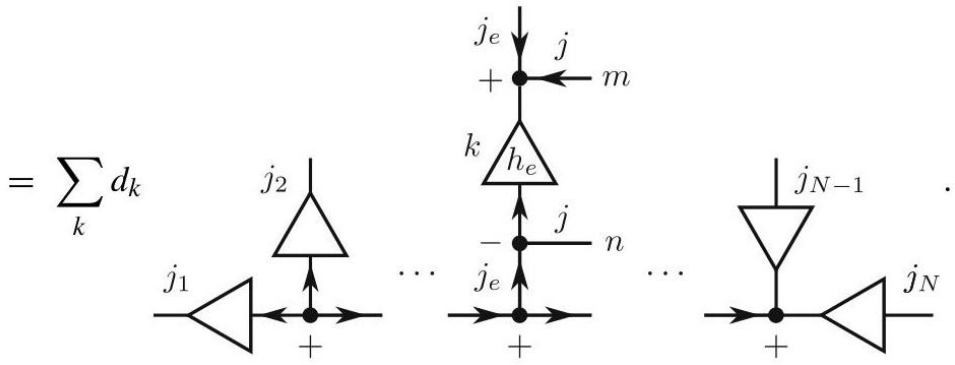

(81)

Consider then the left- and right-invariant vector fields. We want to obtain a graphical expression for the action of the operators $\hat{L}^{(e)}_i$ and $\hat{R}^{(e)}_i$ on the function $T^{v}_{\gamma \mathbf{j},\iota}\left(h_{e_1},\dots,h_{e_N}\right)$. As the action of the left- and right-invariant vector fields on a representation matrix is given by Eqs. (78) and (79), it suffices to recall the graphical representation of the $SU(2)$ generators $\tau^{(j)}_i$ from Eq. (31) to cast the action of these operators into graphical form. Applying this to the state represented by the diagram (80), we establish that the action of the left- and right-invariant vector fields on a spin network vertex is given by the graphical expression

接下来考虑左不变和右不变向量场。我们想要得到算子 $\hat{L}^{(e)}_i$ 和 $\hat{R}^{(e)}_i$ 作用在函数 $T^{v}_{\gamma \mathbf{j},\iota}\left(h_{e_1},\dots,h_{e_N}\right)$ 上的图形表达式。由于左右不变向量场作用在表示矩阵上的结果由式 (78) 和 (79) 给出，我们只需回顾式 (31) 中 $SU(2)$ 生成元 $\tau^{(j)}_i$ 的图形表示，即可将这些算子的作用改写为图形形式。将其应用到图 (80) 表示的态上，我们得到: 左右不变向量场作用在自旋网络顶点上的结果由下述图形表达式给出

$$\hat{L}_i^{(e)} T^v_{\gamma,\mathbf{j},\boldsymbol{\iota}} \;=\; -W_{j_e}$$

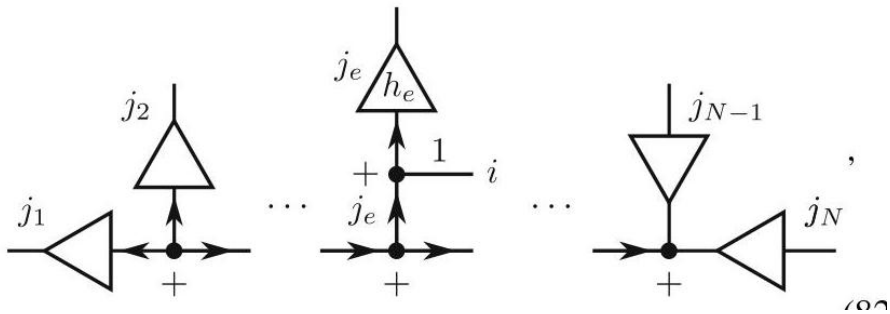

(82)

and

和

$$\hat{R}_i^{(e)} T^v_{\gamma,\mathbf{j},\boldsymbol{\iota}} \;=\; W_{j_e}$$

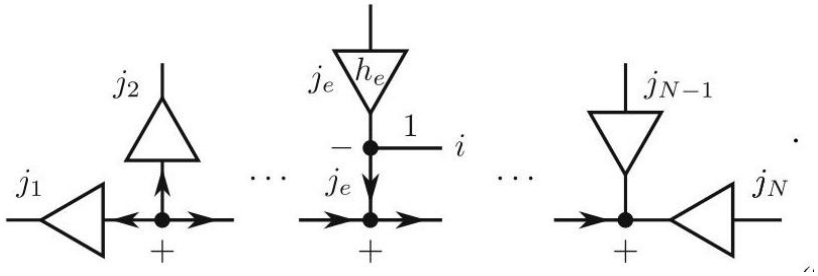

(83)

Note that there is a certain sense of consistency between the invariant vector fields and the orientation of the edge on which they act. If a left-invariant vector field is applied to an outgoing edge, or a right-invariant vector field to an incoming edge, the action of the operator is localized to the vertex v and can be interpreted essentially as an action on just the intertwiner ι_v .

注意，不变向量场与其作用的边的取向之间存在一定的一致性。若左不变向量场作用在出边上，或右不变向量场作用在入边上，算子的作用就局限在顶点 v，本质上可以理解为仅作用在交缠子 ι_v 上。

Equations (81)-(83) provide the graphical representation of the elementary operators of loop quantum gravity. The action of any well-defined operator on a spin network state can now be computed graphically by applying these equations together with the basic rules of graphical calculus presented in sections ”Elements of Graphical Calculus” and ”Calculating with Graphical Diagrams.”

式 (81)-(83) 给出了圈量子引力中基本算子的图形表示。任意良定义算子作用在自旋网络态上的结果，现在都可以结合这些式子与“图形计算基础”和“图形图解计算”两节给出的图形计算基本规则，通过图形方法计算得到。

Example: Matrix Elements of the Hamiltonian Constraint

示例: 哈密顿约束的矩阵元

The task of computing the matrix elements of the Hamiltonian constraint, which is the operator governing the dynamics in the canonical formulation of loop quantum gravity, is a typical example of a calculation which can be performed quite efficiently using the graphical methods presented in this chapter. As an example, let us take a look at a version of the Hamiltonian introduced in [52]. The operator is a slight variation of Thiemann's well-known construction [45], and it has been studied, e.g., in [55] to investigate the consistency between the canonical and covariant formulations of the dynamics in loop quantum gravity.

计算哈密顿约束 (圈量子引力正则形式中支配动力学的算符) 的矩阵元，是使用本章介绍的图形方法就能相当高效完成的典型计算示例。下面我们就以文献 [52] 中介绍的一种哈密顿形式为例进行讲解。该算符是对著名的 Thiemann 构造 [45] 的微小修改，已有研究 (例如文献 [55]) 用它来检验圈量子引力中动力学的正则形式与协变形式的自洽性。

The operator corresponds to the Euclidean part of the Hamiltonian constraint and restricted to a given vertex v of a spin network state; it takes the form

该算符对应哈密顿约束的欧几里得部分，且限制在自旋网络态的给定顶点 v 上；其形式如下

$$\widehat{H}^{\mathrm{E}}_{v} = \sum_{e_I, e_J \text{ at } v} \varepsilon^{ijk} \operatorname{Tr}\left(\tau_k^{(l)} D^{(\hat{l})}\left(\widehat{h_{\alpha_{IJ}}}\right)\right) \hat{J}_i^{(e_I)} \hat{J}_j^{(e_J)} \widehat{V_v^{-1}}. \tag{84}$$

Here $h_{\alpha_{IJ}}$ is the holonomy around the closed triangular loop $\alpha_{IJ} = s_I^{-1} \circ a_{IJ} \circ s_J$, where s_I and s_J are short segments of the edges e_I and e_J starting from v , and a_{IJ} is an arc connecting the endpoint of s_J to the endpoint of s_I . Moreover, each $\hat{J}_i^{(e)}$ denotes either a left- or a right-invariant vector field, according to whether the corresponding edge is oriented outward or inward at the vertex - see the remark below Eq. (83) - and V_v^{-1} is a regularized inverse volume operator (see, e.g., [13, 55]). For the purposes of our example, we will ignore the inverse volume operator, whose action is not accessible by purely graphical means, and focus on the remaining part of operator (84):

其中 $h_{\alpha_{IJ}}$ 是闭合三角形回路 $\alpha_{IJ} = s_I^{-1} \circ a_{IJ} \circ s_J$ 周围的全纯，s_I 和 s_J 是起始于 v 的边 e_I 和 e_J 的短段，a_{IJ} 是连接 s_J 端点与 s_I 端点的弧。此外，每个 $\hat{J}_i^{(e)}$ 表示左不变或右不变向量场，具体取决于对应边在顶点处的指向是向外还是向内——参见式 (83) 下方的注释——而 V_v^{-1} 是正则化的逆体积算符 (参见例如文献 [13, 55])。为了完成本次示例计算，我们将忽略逆体积算符，它的作用无法仅通过图形方法得到，我们将聚焦于算符 (84) 的剩余部分:

$$\widehat{h}^{\mathrm{E}}_{v,e_I,e_J} = \varepsilon^{ijk} \operatorname{Tr}\left(\tau_k^{(l)} D^{(l)}\left(\widehat{h_{\alpha_{IJ}}}\right)\right) \hat{J}_i^{(e_I)} \hat{J}_j^{(e_J)}. \tag{85}$$

Our goal is to calculate the action of the operator $\widehat{h}^{\mathrm{E}}_{v,e_1,e_2}$ on a four-valent spin network vertex. For simplicity, assume that all the edges are oriented outwards from the vertex. Then the relevant part of the spin network function has the form

我们的目标是计算算符 $\widehat{h}^{\mathrm{E}}_{v,e_1,e_2}$ 在四价自旋网络顶点上的作用。为简化起见，假设所有边都从顶点向外定向。那么自旋网络函数的相关部分形式如下

j_1 j_4
e_1

$$D^{(j_1)m_1}{}_{n_1}\left(h_{e_1}\right)\cdots D^{(j_4)m_4}{}_{n_4}\left(h_{e_4}\right)\left(\iota_k^{(j_1\cdots j_4)}\right)^{n_1\cdots n_4} =$$

k

$++$

e_3

$j_2\ j_3$

(86)

where we have chosen a basis of intertwiners where the edges e_1 and e_2 , on which the operator $\widehat{h}^{\mathrm{E}}_{v,e_1,e_2}$ will act, are coupled to the internal spin of the intertwiner. (In the name of readability, we commit a slight abuse of notation by using the edges e_I instead of the holonomies h_{e_I} to label the triangles in the diagram representing the spin network state.)

其中我们选取了 intertwinner 基，算符 $\widehat{h}^{\mathrm{E}}_{v,e_1,e_2}$ 作用的边 e_1 和 e_2 在该基下耦合到 intertwinner 的内自旋。(为了可读性，我们略微滥用了记号: 在表示自旋网络态的图中，我们用边 e_I 代替全纯 h_{e_I} 来标记三角形。)

Each $\hat{J}_i^{(e)}$ in Eq. (85) will now be a left-invariant vector field. Using Eq. (82) to evaluate the action of these operators on the state (86), and appending the diagram

式 (85) 中的每个 $\hat{J}_i^{(e)}$ 现在都是左不变向量场。利用式 (82) 计算这些算符在态 (86) 上的作用，再将图

(87)

$$\varepsilon^{ijk}(\tau_k^{(l)})^m{}_n \;=\; -\sqrt{6}W_l$$

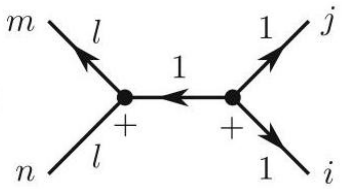

to the resulting expression, we obtain

附加到结果表达式中，我们得到

$$\varepsilon^{ijk}\left(\tau_k^{(l)}\right)^m{}_n \hat{J}_i^{(e_1)}\hat{J}_j^{(e_2)}\left|T^v_{\mathbf{j},k}\right\rangle = -\sqrt{6}W_{j_1}W_{j_2}W_l$$

(88)

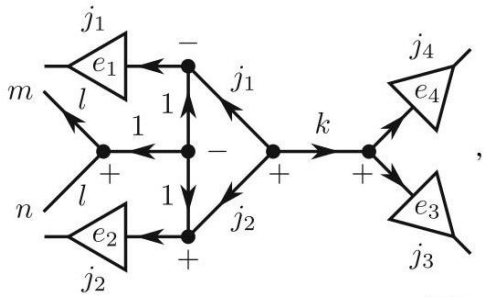

where $\left|T^{v}_{\mathbf{j},k}\right\rangle$ denotes the state (86). We must then bring in the operator $D^{(l)n}{}_{m}\left(h_{\alpha_{12}}\right)$. Using the multiplicative property (73) of the holonomy, we can break this down as

其中 $\left|T^{v}_{\mathbf{j},k}\right\rangle$ 表示态 (86)。接下来我们需要引入算符 $D^{(l)n}{}_{m}\left(h_{\alpha_{12}}\right)$。利用全纯的乘法性质 (73)，我们可以将其分解为

$$D^{(l)n}{}_{m}\left(h_{\alpha_{12}}\right) = D^{(l)n_{n'}}\left(h_{s_1}^{-1}\right) D^{(l)n'm'}\left(h_{a_{12}}\right) \overbrace{D^{(l)m'}{}_{m}\left(h_{s_2}\right)}^{D^{(l)n'}{}_{m}\left(h_{s_2}\right)=D^{(l)m'}{}_{m}\left(h_{s_2}\right).} \tag{89}$$

The action of the rightmost holonomy operator on the holonomy $D^{(j_2)}\left(h_{e_2}\right)$ can be derived by splitting the edge e_2 into the segment s_2 and the remainder e_2' - recall Eq. (73) - and applying Eq. (81). After slightly adjusting the direction of the arrows, we find

最右侧全纯算符在全纯 $D^{(j_2)}\left(h_{e_2}\right)$ 上的作用可以这样推导: 将边 e_2 拆分为段 s_2 和剩余部分 e_2' ——回顾式 (73)——再应用式 (81)。对箭头方向稍作调整后，我们得到

j_2 j_2 j_2
$D^{(l)m'}{}_{m}\left(h_{s_2}\right)$ e_2
=
$D^{(l)m'}{}_{m}\left(h_{s_2}\right)$ s_2
m' m
j_2
l
l_2
l
j_2
S2
+(90)

The operator $D^{(l)n}{}_{n'}\left(h_{s_1}^{-1}\right)$ can be treated in the same way, using Eq. (11) for the matrix elements of the inverse matrix and taking into account the arrows arising from the epsilon tensors. Finally, the holonomy

算符 $D^{(l)n}{}_{n'}\left(h_{s_1}^{-1}\right)$ 可以用同样的方式处理，利用逆矩阵矩阵元的式 (11)，并考虑由 epsilon 张量产生的箭头。最后，全纯

(91)

$D^{(l)n'}{}_{m'}(h_{a_{12}})$ =

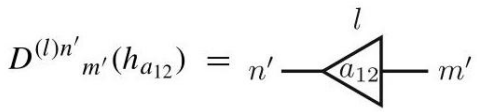

is attached to the diagram. In the end we have

被附加到图中。最终我们得到

$$\widehat{h}^{\mathrm{E}}_{v,e_1,e_2}\left|T^{v}_{\mathbf{j},k}\right\rangle = -\sqrt{6}W_{j_1}W_{j_2}W_{l}$$

$$\times \sum_{l_1,l_2} d_{l_1} d_{l_2} (-1)^{2l_1+2l_2}$$

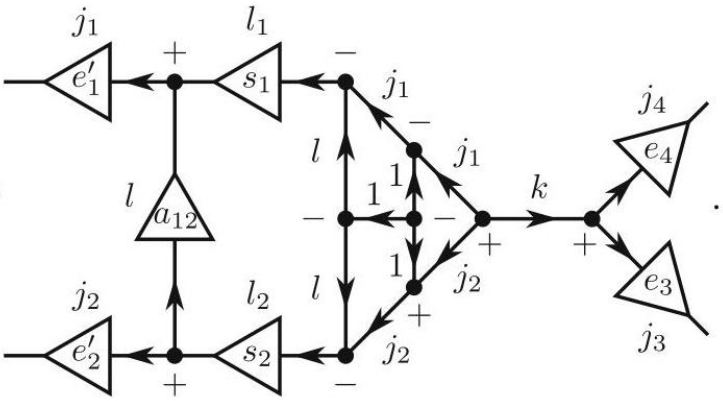

(92)

The next step is to express the result in terms of known quantities such as $6j$ - symbols with the help of the fundamental theorem. We begin by applying Eq. (59) to the three-valent invariant tensor within the above diagram, thus finding that the diagram is equal to

下一步是利用基本定理，将结果表示为 $6j$ 符号这类已知量的形式。我们首先将式 (59) 应用于上图中的三价不变张量，由此得到该图等于

(93)

$$f(j_1, j_2, k, l, l_1, l_2)$$

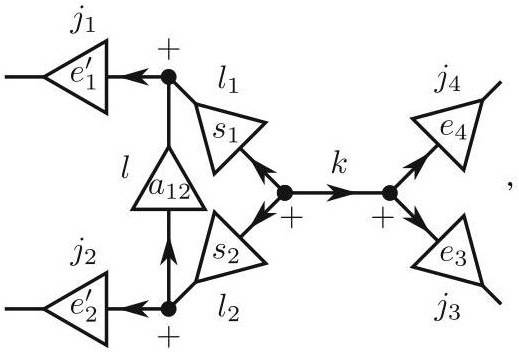

where

其中

(94)

$$f(j_1, j_2, k, l, l_1, l_2) =$$

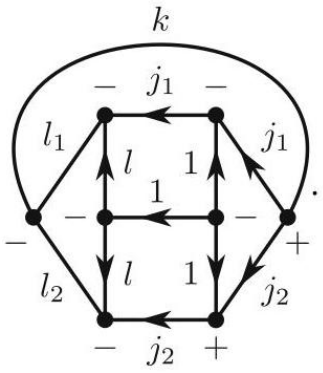

This diagram can be recognized as the so-called $12j$ -symbol of the second kind (see, e.g., [49,56]), but we may equally well continue to use the fundamental theorem to break it down. Clearly the diagram cannot be split into two disconnected pieces by cutting only three lines. If we cut the four lines connecting the central part of the diagram to the two outer nodes, as indicated by Eq. (65), we see that

该图就是所谓的第二类 $12j$ 符号 (例如参见文献 [49,56]), 不过我们也可以继续利用基本定理对其分解。显然, 仅切割三条线无法将该图拆分为两个不连通部分。如果我们按照式 (65) 标注的方式, 切割连接图中心部分和两个外节点的四条线, 可得

$$\widehat{h}^{\mathrm{E}}_{v,e_1,e_2}\left|T^{v}_{\mathbf{j},k}\right\rangle = \sqrt{6}W_{j_1}W_{j_2}W_{l}\sum_{l_1,l_2,x} d_{l_1}d_{l_2}d_x(-1)^{k+l_1-l_2}$$

$$\times\begin{Bmatrix} j_1 & j_2 & k \\ l_2 & l_1 & x \end{Bmatrix}\begin{Bmatrix} j_1 & j_1 & 1 \\ x & l & l_1 \end{Bmatrix}\begin{Bmatrix} j_2 & j_2 & 1 \\ x & l & l_2 \end{Bmatrix}\begin{Bmatrix} 1 & 1 & 1 \\ x & l & l \end{Bmatrix}\left|\widetilde{T}^{v}_{\mathbf{j},\mathbf{l},k}\right\rangle \tag{96}$$

$$f(j_1, j_2, k, l, l_1, l_2) = \sum_x d_x$$

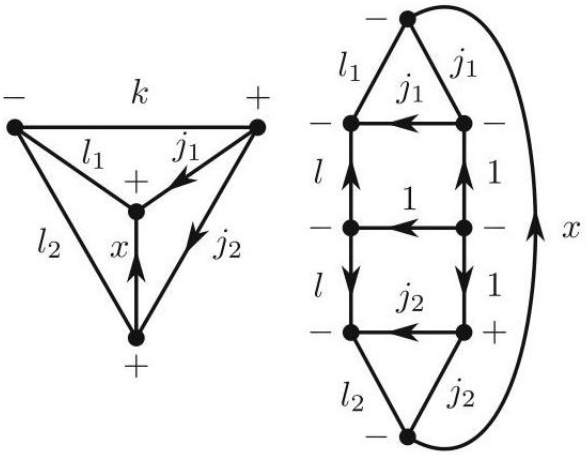

(95)

Here the first piece is immediately recognizable as a $6j$ -symbol, while the second piece can be reduced to a product of three $6j$ -symbols by making two horizontal cuts. After simplifying the factors of (-1) , we obtain the final result of our calculation in the form

此处第一个部分可直接识别为一个 $6j$ 符号，而第二个部分通过两次水平切割可约化为三个 $6j$ 符号的乘积。化简 (-1) 因子后，我们得到计算的最终结果形式为

where $\left|\widetilde{T}^{\upsilon}_{\mathbf{j},\mathbf{l},k}\right\rangle$ is the state defined by the diagram in Eq. (93).

其中 $\left|\widetilde{T}^{\upsilon}_{\mathbf{j},\mathbf{l},k}\right\rangle$ 是式 (93) 中该图定义的态。

Summary

摘要

In this chapter we have presented an introduction to the graphical calculus of $SU(2)$, which constitutes a highly efficient technique for calculations involving $SU(2)$ recoupling theory. The graphical formalism, which has been originally introduced in the literature as a method for dealing with calculations in the quantum theory of angular momentum, is built out of two key ingredients: (1) a graphical notation consisting of diagrammatic representations of the elementary objects of $SU(2)$ recoupling theory, such as Clebsch-Gordan coefficients, Wigner nj-symbols, and Wigner matrices, and (2) the basic properties satisfied by these graphical diagrams, which follow from the properties of the corresponding non-graphical objects and which promote the graphical notation into a powerful diagrammatic calculus. In particular, in section "Calculating with Graphical Diagrams" we introduced a set of graphical identities which we named the fundamental theorem of graphical calculus; these identities provide an essential tool for simplifying complicated graphical diagrams.

本章我们介绍了 $SU(2)$ 图形演算，它是处理涉及 $SU(2)$ 重耦合理论计算的高效方法。该图形形式最初作为角动量量子理论的计算方法被提出，由两个核心部分构成:(1) 图形记号，用 diagrams 表示 $SU(2)$ 重耦合理论的基本对象，例如 Clebsch-Gordan 系数、Wigner n-j 符号、Wigner 矩阵；(2) 这些图形满足的基本性质，这些性质源于对应非图形对象的性质，也让该图形记号发展为强大的图解演算。特别地，我们在「图形计算」一节引入了一组图形恒等式，将其命名为图形演算基本定理；这些恒等式是简化复杂图形的核心工具。

In the graphical approach, any given algebraic expression in $SU(2)$ recoupling theory is represented in a definite and unambiguous way by a corresponding graphical formula. Calculations can then be performed graphically by following a set of straightforward rules for manipulating graphical diagrams. The resulting transformations of the graph correspond uniquely to algebraic manipulations of the corresponding non-graphical expressions, so any calculation performed by the graphical method can also be performed by conventional algebraic techniques. However, the graphical form of the calculation is usually considerably more concise, efficient, and visually easier to follow.

在图形方法中，$SU(2)$ 重耦合理论里任意给定的代数表达式都可以被对应图形公式明确无歧义地表示。我们只需遵循一组简单直接的规则操作图形，就能完成计算。图的变换唯一对应对应非图形表达式的代数操作，因此图形法能完成的计算，传统代数方法同样可以完成，但图形形式的计算通常要简洁得多、效率更高，也更便于直观理解。

The graphical calculus of $SU(2)$ provides a very effective practical tool for calculations involving the spin network states of loop quantum gravity, which have the structure of $SU(2)$ representation matrices, associated

with the edges of a graph, contracted with intertwiners, or invariant tensors of $SU(2)$, associated with the vertices of the graph. By applying the basic definitions of the graphical formalism, the action of the elementary operators of loop quantum gravity can be cast into a graphical form. Given an operator constructed out of holonomy and flux operators, the action of the operator on spin network states can then be systematically computed by applying the rules of graphical calculus. As a concrete example, we considered the calculation of the matrix elements of a particular version of the Hamiltonian constraint operator in the spin network basis. Many more examples of the use of graphical calculus in loop quantum gravity can be found in the articles cited in the bibliography, where graphical techniques have been successfully applied to a variety of physically relevant and technically quite nontrivial calculations.

$SU(2)$ 图形演算是计算圈量子引力自旋网络态非常有效的实用工具，自旋网络态的结构为: 图的边关联 $SU(2)$ 表示矩阵，图的顶点关联 $SU(2)$ 的交缠子 (即不变张量)，再将这些表示矩阵缩并得到自旋网络态。利用图形形式的基本定义，圈量子引力基本算符的作用可以被改写为图形形式。对于任意一个由和乐算符和通量算符构造出的算符，我们都可以通过应用图形演算规则，系统地计算该算符作用在自旋网络态上的结果。作为具体实例，我们计算了自旋网络基下特定形式哈密顿约束算符的矩阵元。更多图形演算在圈量子引力中应用的例子可以在参考文献所列文章中找到，这些文献已经将图形技术成功应用于多种物理相关、技术上相当复杂的计算中。

Cross-References

交叉引用

Emergence of Riemannian Quantum Geometry

黎曼量子几何的涌现

Hamiltonian Theory: Dynamics

哈密顿理论: 动力学

- Loop Quantum Gravity and Quantum Information

- 圈量子引力与量子信息

Spin Foams: Foundations

自旋泡沫: 基础

Spinfoams and High-Performance Computing

自旋泡沫与高性能计算

Acknowledgments I. M. acknowledges support of the National Science Centre, Poland, through grants no. 2018/30/Q/ST2/00811 and 2022/44/C/ST2/00023. J. Y. is supported in part by NSFC Grants No. 12165005 and No. 11961131013.

致谢波兰国家科学中心通过编号 2018/30/Q/ST2/00811 和 2022/44/C/ST2/00023 的项目资助了 I. M.。J. Y. 部分得到了国家自然科学基金项目编号 12165005 和 11961131013 的支持。

References

参考文献

1. E. Alesci, F. Cianfrani, Phys. Rev. D 87, 083521 (2013). [arXiv:1301.2245]
2. E. Alesci, F. Cianfrani, Phys. Rev. D 90, 024006 (2014). [arXiv:1402.3155]
3. E. Alesci, C. Rovelli, Phys. Rev. D 76, 104012 (2007). [arXiv:0708.0883]
4. E. Alesci, C. Rovelli, Phys. Rev. D 82, 044007 (2010). [arXiv:1005.0817]
5. E. Alesci, T. Thiemann, A. Zipfel, Phys. Rev. D 86, 024017 (2012). [arXiv:1109.1290]
6. E. Alesci, K. Liegener, A. Zipfel, Phys. Rev. D 88, 084043 (2013). [arXiv:1306.0861]
7. E. Alesci, M. Assanioussi, J. Lewandowski, I. Mäkinen, Phys. Rev. D 91, 124067 (2015). [arXiv:1504.02068]
8. A. Ashtekar, J. Lewandowski, Adv. Theor. Math. Phys. 1, 388 (1997). [arXiv:gr-qc/9711031]
9. A. Ashtekar, J. Lewandowski, Class. Quant. Grav. 21, R53 (2004). [arXiv:gr-qc/0404018]
10. A. Ashtekar, J. Pullin (eds.), Loop Quantum Gravity: The First 30 Years (World Scientific Publishing, Singapore, 2017)
11. J.C. Baez, Lect. Notes Phys. 543, 25 (2000). [arXiv:gr-qc/9905087]
12. J.W. Barrett, I. Naish-Guzman, Class. Quant. Grav. 26, 155014 (2009). [arXiv:0803.3319]
13. E. Bianchi, Nucl. Phys. B 807, 591 (2009). [arXiv:0806.4710]
14. R. Borissov, S. Major, L. Smolin, Class. Quant. Grav. 13, 3183 (1996). [arXiv:gr-qc/9512043]
15. R. Borissov, R. De Pietri, C. Rovelli, Class. Quant. Grav. 14, 2793 (1997). [arXiv:gr-qc/9703090]
16. D.M. Brink, G.R. Satchler, Angular Momentum (Clarendon Press, Oxford, 1968)
17. R. De Pietri, C. Rovelli, Phys. Rev. D 54, 2664 (1996). [arXiv:gr-qc/9602023]
18. B. Dittrich, M. Geiller, New. J. Phys 19, 013003 (2017). [arXiv:1604.05195]
19. P. Dona, P. Frisoni, Universe 8, 208 (2022). [arXiv:2202.04360]
20. P. Dona, F. Gozzini, G. Sarno, Phys. Rev. D 102, 106003 (2020). [arXiv:2004.12911]
21. A.R. Edmonds, Angular Momentum in Quantum Mechanics (Princeton University Press, Princeton, 1974)
22. J. Engle, E. Livine, R. Pereira, C. Rovelli, Nucl. Phys. B 799, 136 (2008). [arXiv:0711.0146]
23. M. Fecko, Differential Geometry and Lie Groups for Physicists (Cambridge University Press, Cambridge, 2006)
24. L. Freidel, K. Krasnov, Class. Quant. Grav. 25, 125018 (2008). [arXiv:0708.1595]
25. P. Frisoni, F. Gozzini, F. Vidotto, Phys. Rev. D 105, 106018 (2022). [arXiv:2112.14781]
26. M. Gaul, C. Rovelli, Class. Quant. Grav. 18, 1593 (2001). [arXiv:gr-qc/0011106]
27. K. Giesel, H. Sahlmann, Proc. Sci. QGQGS2011, 002 (2011). [arXiv:1203.2733]
28. M. Han, Y. Ma, W. Huang, Int. J. Mod. Phys. D 16, 1397 (2007). [arXiv:gr-qc/0509064]
29. W. Kamiński, M. Kisielowski, J. Lewandowski, Class. Quant. Grav. 27, 095006 (2010). [arXiv:0909.0939]
30. L.H. Kauffman, S.L. Lins, Temperley-Lieb Recoupling Theory and Invariant of 3-Manifolds (Princeton University Press, Princeton, 1994)
31. N. Kawamoto, N. Sato, Y. Uchida, Nucl. Phys. B 574, 809 (2000). [arXiv:hep-th/9911228]
32. K. Liegener, T. Thiemann, Phys. Rev. D 94, 024042 (2016). [arXiv:1605.05975]
33. Y. Ling, L. Smolin, Phys. Rev. D 61, 044008 (2000). [arXiv:hep-th/9904016]

34. P. Martin-Dussaud, Gen. Rel. Grav. 51, 110 (2019). [arXiv:1902.08439]

35. I. Mäkinen, Ph.D. thesis, University of Warsaw, 2019. [arXiv:1910.06821]

36. I. Mäkinen, [arXiv:1910.06821]

37. R. Penrose, W. Rindler, Spinors and Space-Time, Two-Spinor Calculus and Relativistic Fields, vol. 1 (Cambridge University Press, Cambridge, 1984)

38. A. Perez, Living Rev. Rel. 16, 3 (2013). [arXiv:1205.2019]

39. G. Ponzano, T. Regge, Semiclassical Limit of Racah Coefficients, in Spectroscopic and Group Theoretical Methods in Physics, eds. by F. Bloch et al. (North-Holland, Amsterdam, 1968)

40. C. Rovelli, Quantum Gravity (Cambridge University Press, Cambridge, 2004)

41. C. Rovelli, Proc. Sci. QGQGS2011, 003 (2011). [arXiv:1102.3660]

42. C. Rovelli, L. Smolin, Nucl. Phys. B 442, 593 (1995). [arXiv:gr-qc/9411005]

43. C. Rovelli, L. Smolin, Phys. Rev. D 52, 5743 (1995). [arXiv:gr-qc/9505006]

44. C. Rovelli, F. Vidotto, Covariant Loop Quantum Gravity: An Elementary Introduction to Quantum Gravity and Spinfoam Theory (Cambridge University Press, Cambridge, 2014)

45. T. Thiemann, Class. Quant. Grav. 15, 839 (1998). [arXiv:gr-qc/9606089]

46. T. Thiemann, Lect. Notes Phys. 631, 41 (2003). [arXiv:gr-qc/0210094]

47. T. Thiemann, Modern Canonical Quantum General Relativity (Cambridge University Press, Cambridge, 2007)

48. T. Thiemann, A. Zipfel, Class. Quant. Grav. 31, 125008 (2014). [arXiv:1307.5885]

49. D.A. Varshalovich, A.N. Moskalev, V.K. Khersonsky, Quantum Theory of Angular Momentum: Irreducible Tensors, Spherical Harmonics, Vector Coupling Coefficients, 3nj Symbols (World Scientific, Singapore, 1988)

50. E.P. Wigner, Group Theory and Its Application to the Quantum Mechanics of Atomic Spectra (Academic Press Inc., New York, 1959)

51. J. Yang, Y. Ma, Eur. Phys. J. C 77, 235 (2017). [arXiv:1505.00223; arXiv:1505.00225]

52. J. Yang, Y. Ma, Phys. Lett. B 751, 343 (2015). [arXiv:1507.00986]

53. J. Yang, Y. Ma, Phys. Rev. D 94, 044003 (2016). [arXiv:1602.08688]

54. J. Yang, Y. Ma, Chin. Phys. C 43, 103106 (2019). [arXiv:1908.10600]

55. J. Yang, C. Zhang, Y. Ma, Phys. Rev. D 104, 044025 (2021). [arXiv:2102.05881]

56. A.P. Yutsis, I.B. Levinson, V.V. Vanagas, Mathematical Apparatus of the Theory of Angular Momentum (Israel Program for Scientific Translation, Jerusalem, 1962)